Data report: clay mineral assemblages in the Shikoku Basin, NanTroSEIZE subduction inputs, IODP Sites C0011 and C0012[1]

Michael B. Underwood[2] and Junhua Guo[2]

Chapter contents

Abstract

This report documents clay mineral assemblages outboard of the Nankai Trough at two sites in the Shikoku Basin. The sites make up part of the Kumano transect, offshore south-central Japan. Coring began during Integrated Ocean Drilling Program (IODP) Expedition 322, as part of the Nankai Trough Seismogenic Zone Experiment (NanTroSEIZE). IODP Site C0011 is located on the northwest flank of Kashinosaki Knoll, and IODP Site C0012 is located on the summit of the seamount. A total of 292 samples of hemipelagic mud and mudstone were analyzed by X-ray diffraction, using oriented aggregates of the clay-size fraction (<2 µm). Smectite varies the most among the clay-size constituents, ranging in abundance from 35% to 100% (where smectite + illite + chlorite + kaolinite + quartz = 100%). Specimens with smectite contents of 80% or more are classified as bentonites, and we identified 44 such samples. The estimated amount of smectite in bulk mudstone ranges from 24% to 87% (where total clay minerals + quartz + feldspar + calcite = 100%), and a substantial number of bulk samples contain >45% smectite. On average, the expandability of illite/smectite mixed-layer clay is equal to 77%, and the average proportion of illite in illite/smectite is 11%. There is no systematic progression of clay mineral diagenesis over the depths sampled. Most values of illite crystallinity index are consistent with a detrital source that contains sedimentary rocks that were exposed to anchizone conditions of incipient metamorphism. The smectite-rich clay mineral assemblage is typical of early to middle Miocene deposits within the lower part of the Shikoku Basin.

Introduction

The Nankai Trough subduction zone is the product of convergence between the Philippine Sea plate and the Eurasian plate (Fig. F1). Many sites have been drilled and cored in this region over the past four decades, including sites from Deep Sea Drilling Project (DSDP) Legs 31 and 87 (Karig, Ingle, et al., 1975; Kagami, Karig, Coulbourn, et al., 1986) and Ocean Drilling Program (ODP) Legs 131, 190, and 196 (Taira et al., 1992; Moore et al., 2001, 2005). Integrated Ocean Drilling Program (IODP) Expeditions 314, 315, and 316 focused on a new transect—the Kumano transect—during Stage 1 of the Nankai Trough Seismogenic Zone Ex-

[1]Underwood, M.B., and Guo, J., 2013. Data report: clay mineral assemblages in the Shikoku Basin, NanTroSEIZE subduction inputs, IODP Sites C0011 and C0012. *In* Saito, S., Underwood, M.B., Kubo, Y., and the Expedition 322 Scientists, *Proc. IODP,* 322: Tokyo (Integrated Ocean Drilling Program Management International, Inc.).
doi:10.2204/iodp.proc.322.202.2013
[2]Department of Geological Sciences, University of Missouri, Columbia MO, USA. Correspondence author: underwoodm@missouri.edu

periment (NanTroSEIZE) (Ashi et al., 2009; Screaton et al., 2009; Tobin et al., 2009). Subsequent drilling during IODP Expedition 322 concentrated on inputs to the subduction zone by coring two sites in the Shikoku Basin (see the "Expedition 322 summary" chapter [Underwood et al., 2010]). IODP Sites C0011 and C0012 are located on the northwest flank and at the summit of a subducting basement high known as Kashinosaki Knoll (Ike et al., 2008) (Fig. F2).

Previous investigations of clay minerals in the vicinity of the Nankai Trough and the Shikoku Basin demonstrated that the hemipelagic mud(stones) change in composition largely as function of depositional age (Cook et al., 1975; Chamley, 1980; Chamley et al., 1986; Fagel et al., 1992; Underwood et al., 1993a, 1993b; Steurer and Underwood, 2003; Underwood and Steurer, 2003). Underwood (2007) summarized findings from the so-called reference sites along the Muroto and Ashizuri transects (ODP Sites 1173 and 1177) (Fig. F1), which are of particular interest for comparisons with Sites C0011 and C0012. Miocene strata throughout the Nankai-Shikoku region tend to contain higher percentages of smectite, whereas Pliocene and Pleistocene deposits are more enriched in illite and chlorite. This temporal trend also exists in the shallow accretionary prism and forearc basin of the Kumano transect (Guo and Underwood, 2012).

The abundance and hydration state of expandable clay minerals are important factors to consider during the NanTroSEIZE project because of their influence on fluid production as depth increases along the plate interface (Saffer et al., 2008). Clay diagenesis (particularly the smectite-to-illite reaction) is more advanced along the Muroto transect (Site 1173), where proximity to the paleospreading center of the subducting Shikoku Basin is responsible for higher heat flow (Underwood and Pickering, 1996; Masuda et al., 1996, 2001; Steurer and Underwood, 2003; Spinelli and Underwood, 2005; Saffer et al., 2008). In contrast, there is no evidence for presubduction diagenesis at Site 1177 (Steurer and Underwood, 2003). To document clay composition in the Kumano transect area, particularly for those stratigraphic units that eventually affect conditions near the subduction megathrust, we analyzed the clay mineral assemblages from 292 samples of hemipelagic mud and mudstone using X-ray diffraction (XRD). This report documents how the common clay minerals (smectite, illite, chlorite, and kaolinite) change in relative abundance as a function of depositional age and lithostratigraphy. We also test whether or not smectite-to-illite diagenesis has progressed to any measurable extent prior to the arrival of sedimentary strata at the subduction front.

Methods

Calculations of mineral abundance

Marine sediment samples can be analyzed by XRD using a variety of techniques. For example, the presence of a specific detrital and/or authigenic mineral can be detected easily through visual recognition of characteristic (hkl) peak positions. It is more challenging, however, to estimate the relative abundance of a mineral in bulk sediment or in the clay-size fraction with meaningful accuracy (e.g., Moore, 1968; Heath and Pisias, 1979; Johnson et al., 1985). The most common approach for analyzing clays in marine geology has been to multiply the Biscaye (1965) weighting factors by the peak areas of basal reflections and normalize to 100% (McManus, 1991). Errors can be substantial, however, and accuracy of calculated values is affected by the absolute abundance by weight of each mineral in the mixture (Underwood et al., 2003). XRD results also change depending on sample disaggregation technique, chemical pretreatments, particle size separation, crystallinity and chemical composition of minerals, peak-fitting algorithms, and the degree of preferred orientation of crystallites (e.g., Moore and Reynolds, 1989; Ottner et al., 2000). Even though data reproducibility might be very good, accuracy is usually no better than ±10% unless the analytical methods include calibration with internal standards, use of single-line reference intensity ratios, and some fairly elaborate sample preparation steps to create random particle orientations (Środoń et al., 2001; Omotoso et al., 2006).

One goal of NanTroSEIZE is to obtain internally consistent, semiquantitative estimates of mineral abundance in the clay-size fraction for a large number of samples. To accomplish this, we use a matrix of singular value decomposition (SVD) normalization factors, as documented in full detail by Underwood et al. (2003). Figure F3 shows representative X-ray diffractograms for two clay-size aggregates from the Shikoku Basin. The matrix of SVD factors (Table T1) is applied to the integrated areas of a broad smectite (001) peak centered at ~5.3°2θ (d-value = 16.5 Å), the illite (001) peak at ~8.9°2θ (d-value = 9.9 Å), the composite chlorite (002) + kaolinite (001) peak at 12.5°2θ (d-value = 7.06 Å), and the quartz (100) peak at 20.85°2θ (d-value = 4.26 Å). Average errors for the standard mineral mixtures used to calibrate this method are approximately 3% for smectite, 1% for illite, 2% for chlorite, and 1.4% for quartz (Underwood et al., 2003). Because of the nearly total overlap between the kaolinite (001) and chlorite (002) reflections, we first calculate that relative abundance as undifferentiated chlorite + kaolinite, and then solve for the proportion of each mineral using the double peak at ~25°2θ (Fig. F3) and a refined version of the Biscaye (1964) method, as documented fully by Guo and Underwood (2011). Analysis of standard mineral mixtures shows that the average error for the chlorite/kaolinite ratio is 2.6%. To provide an estimate of the abundance of individual clay minerals in the bulk mudstone, we also multiply each relative percentage among the clay minerals (i.e., excluding quartz) by the weight percent of total clay minerals from shipboard bulk powder XRD analyses of co-located "cluster" specimens (e.g., see the "Site C0011" chapter [Expedition 322 Scientists, 2010a]). To facilitate comparisons with many of the other published data sets from the region, data tables include weighted peak area percentages for smectite, illite, chlorite, and kaolinite using Biscaye (1965) weighting factors. These values are relative percentages and should be regarded as semiquantitative.

To characterize the extent of clay diagenesis, we used the saddle/peak method of Rettke (1981) to calculate the percent expandability of smectite and illite/smectite (I/S) mixed-layer clay. This method is sensitive to the proportions of discrete illite (I) versus I/S mixed-layer clay. Our calculations follow a curve for 1:1 mixtures of I and I/S. A complementary way to calculate the proportion of illite in the I/S mixed-layer phase is based on the position (d-value) of the (002/003) peak (following Moore and Reynolds, 1989) after correcting the diffractogram peaks for misalignment of the detector and sample holder. We also report values of illite crystallinity index as the peak width measured at half height (Δ°2θ) for the (001) reflection.

Sample preparation

Isolation of clay-size fractions starts with air drying and gentle hand-crushing of the mud/mudstone with a mortar and pestle, after which specimens are immersed in 3% H_2O_2 for at least 24 h to digest organic matter. We then add ~250 mL of Na hexametaphosphate solution (concentration of 4 g/1000 mL distilled H_2O) and insert the beakers into an ultrasonic bath for several minutes to promote disaggregation and deflocculation. These steps are repeated until disaggregation is complete. Washing consists of two passes through a centrifuge (8200 revolutions per minute [rpm] for 25 min; ~6000 g) with resuspension in distilled-deionized water after each pass. After transferring the suspended sediment to a 60 mL plastic bottle, each sample is resuspended by vigorous shaking and a 2 min application of a sonic cell probe. The clay-size splits (<2 µm spherical equivalent settling diameter) are then separated by centrifugation (1000 rpm for 2.4 min; ~320 g). Oriented clay aggregates are prepared using the filter-peel method (Moore and Reynolds, 1989) and 0.45 µm membranes. The clay aggregates are saturated with ethylene glycol vapor for at least 24 h prior to XRD analysis, using a closed vapor chamber heated to 60°C.

X-ray diffraction parameters

The XRD laboratory at the University of Missouri (USA) utilizes a Scintag Pad V X-ray diffractometer with CuKα radiation (1.54 Å) and a Ni filter. Scans of oriented clay aggregates are run at 40 kV and 30 mA over a scanning range of 3°–26.5°2θ, a rate of 1°2θ/min, and a step size of 0.01°2θ. Slits are 0.5 mm (divergence) and 0.2 mm (receiving). The digital data are processed using MacDiff software (version 4.2.5) to establish a baseline of intensity, smooth counts, correct peak positions offset by misalignment of the detector (using the quartz [100] peak at 20.95°2θ; d-value = 4.24 Å), determine peak intensity (counts/step), and calculate integrated peak areas (total counts). This program also calculates peak width at half height (Δ°2θ).

Results

Almost all of the samples analyzed in this study were selected from co-located clusters immediately adjacent to the whole-round samples used for shipboard analyses of interstitial water chemistry and shore-based tests of frictional, geotechnical, and hydrogeological properties. Each cluster includes a specimen for shipboard bulk powder XRD analysis, which provided estimates of the relative abundance of total clay minerals (see the "Site C0011" and "Site C0012" chapters [Expedition 322 Scientists, 2010a, 2010b]). All of the values of XRD peak-area (total counts) for minerals in the clay-size fraction are tabulated in Table T2. Table T3 lists the calculated values of mineral abundance (weight percent) using SVD normalization factors, as well as area percent using the Biscaye (1965) peak-area weighting factors. Specimens with 80% or more smectite in the clay-size fraction are classified in this report as bentonites. For smectite, we calculated its abundance in the bulk mudstone by multiplying the percentage of smectite within each clay mineral assemblage (where smectite + illite + chlorite + kaolinite = 100%) by the percentage of total clay minerals in the same bulk mudstone (where total clay minerals + quartz + feldspar + calcite = 100%) (for bulk powder data, see the "Site C0011" and "Site C0012" chapters [Expedition 322 Scientists, 2010a, 2010b]). Indicators of clay diagenesis (I/S expandability, percent illite in I/S, and illite crystallinity index) are tabulated in Table T4.

The descriptions below are meant to highlight temporal variations in clay composition organized by lithostratigraphic unit, and Table T5 provides a statistical comparison among the units.

Site C0011

Shipboard scientists during Expedition 322 divided the stratigraphic column at Site C0011 into five lithologic units (see the "Site C0011" chapter [Expedition 322 Scientists, 2010a]). Because of time limitations, sampling began at 340 m core depth below seafloor (CSF) rather than the mudline, and the hole was abandoned ~170 m above the basement total depth target because of premature destruction of the drill bit. The provisional lithologic characterization of Unit I (hemipelagic/pyroclastic facies) was based on logging-while-drilling results, but the upper part of the sedimentary section was eventually verified by coring during IODP Expedition 333 (Expedition 333 Scientists, 2011).

The first cores recovered during Expedition 322 fall within the upper Miocene epoch (~7.6 Ma) and define the top of Unit II (Fig. F4). This volcanic turbidite facies consists of hemipelagic mudstone, sandstone/siltstone turbidites with abundant pyroclastic debris, and mass transport deposits. Smectite is the most abundant clay-size mineral in Unit II (average = 65%) followed by illite (average = 24%). Both of these clay minerals show considerable amounts of scatter. The chlorite + kaolinite content averages 8% within this unit, and clay-size quartz averages 2%. We sampled 11 bentonites within Unit II, and our estimates for the proportion of smectite in the bulk mudstones range from 29% to 87% (average = 42%) (Fig. F5; Table T5).

The dominant lithology of Unit III (hemipelagic facies) is bioturbated mudstone (silty clay to clayey silt); these strata range in age from 9.1 to 12.2 Ma (Fig. F4). Smectite is the dominant clay-size mineral within this unit, making up an average of 59% of the clay-size fraction. Illite content ranges from 10% to 33% (average = 27%). Values of chlorite + kaolinite average 10%, and clay-size quartz content averages 4%. We found two identifiable bentonites within Unit III. Figure F5 shows that smectite abundance in bulk mudstone ranges from 31% to 73% (average = 42%).

Unit IV (silty turbidite facies) is composed of silty claystone, fine-grained siliciclastic sandstone, and siltstone ranging in age from 12.2 to 14.0 Ma (Fig. F4). Core recovery within this unit was incomplete. Smectite (average = 68%) is the most abundant mineral in the clay-size fraction, followed on average by illite (20%), chlorite + kaolinite (7%), and quartz (5%). Unit IV contains five bentonite samples, and smectite abundance in bulk mudstone ranges from 25% to 85% (Fig. F5).

Recovery of Unit V (volcaniclastic facies) was very poor because of technical difficulties, and drilling was terminated at 881 m drilling depth below seafloor (DSF). The estimated depth to the top of basaltic basement is 1050 m seismic depth below seafloor (SSF). Based on limited recovery, the lithology of Unit V includes silicic tuff and tuffaceous sandstone (Fig. F4). Mudstone interbeds contain between 45% and 100% smectite in the clay-size fraction (average = 76%). Average values for illite, chlorite + kaolinite, and quartz are 13%, 4%, and 6%, respectively. The volcaniclastic facies includes seven identifiable bentonites, and smectite abundance in bulk mudstone ranges from 31% to 91% (average = 57%) (Fig. F5).

Figure F6 shows that the expandability of I/S mixed-layer clay minerals does not change significantly from the top of Unit II to base of the cored interval. The average value of I/S expandability is 77%. The proportion of illite in the I/S averages 11% and ranges from 0% to 27%. These plots do not reveal any meaningful progression of smectite-to-illite diagenesis as a function of depth, although it is important to remember that coring terminated ~170 m above the top of igneous basement. Heat flow data collected during Expedition 333 indicate the temperature is equal to ~80°C at the sediment/basalt interface (Expedition 333 Scientists, 2011), so diagenesis could advance to higher proportions of illite in I/S below the deepest core recovery. Values of illite crystallinity index typically range between 0.42 and 0.25 $\Delta°2\theta$. Such values are consistent with erosion of the illite as a detrital constituent from sedimentary source terrains that had been exposed to anchizone conditions of incipient metamorphism (e.g., Blenkinsop, 1988; Kisch, 1990).

Site C0012

Six sedimentary units rest above igneous basement at Site C0012 (Fig. F7), which is positioned at the summit of Kashinosaki Knoll (Fig. F2). The overall trend displayed by clay mineral assemblages shows progressive downsection decreases in illite content coupled with consistent increases in smectite (Fig. F7). Values of smectite also display considerable scatter, particularly within the lower half of the section. The contents of chlorite, kaolinite, and quartz are subsidiary to smectite throughout.

The principal lithology of Unit I (hemipelagic/pyroclastic facies) is hemipelagic mud (silty clay to clayey silt) with numerous interbeds of volcanic ash. Recovery of this unit was poor, however, and drilling disturbance was severe. Consequently, the upper part of the sedimentary section was cored again during Expedition 333 (Expedition 333 Scientists, 2011). Smectite is the most abundant clay-size mineral in Unit I (average = 53%), followed by illite (average = 32%), chlorite + kaolinite (average = 14%), and quartz (average = 1%). We found only one bentonite at the top of this unit (cored during jet-in). Estimates for the proportion of smectite in the bulk mud range from 25% to 56% (average = 36%) (Fig. **F8**; Table **T5**).

The age of Unit II (volcanic turbidite facies) ranges from 7.8 to 9.4 Ma, and the sediment consists of hemipelagic mudstone, sandstone/siltstone turbidites with abundant pyroclastic material, and mass transport deposits (Fig. **F7**). The most abundant clay-size mineral in Unit II is smectite (average = 63%), followed by illite (average = 26%), chlorite + kaolinite (average = 9%), and quartz (average = 2%). We found only one bentonite within this unit. Estimates for the proportion of smectite in the bulk mudstones range from 26% to 62% (average = 43%) (Fig. **F8**; Table **T5**).

The dominant lithology of Unit III (hemipelagic facies) is bioturbated mudstone (silty clay to clayey silt); these homogeneous strata range in age from 9.4 to 12.7 Ma (Fig. **F7**). Smectite is the dominant clay-size mineral within this unit, making up an average of 64% of the clay-size fraction. Illite content ranges from 13% to 35% (average = 25%). Values of chlorite + kaolinite average 8%, and clay-size quartz content averages 5%. We found four identifiable bentonites in the lower portion of Unit III. Smectite abundance in bulk mudstone ranges from 38% to 62% (average = 49%).

Unit IV (silty turbidite facies) is composed of silty claystone, fine-grained siliciclastic sandstone, and siltstone ranging in age from 12.7 to 13.5 Ma (Fig. **F7**). Smectite (average = 66%) is the most abundant mineral in the clay-size fraction, followed on average by illite (21%), chlorite + kaolinite (8%), and quartz (5%). Unit IV contains two bentonites. Smectite abundance in bulk mudstone ranges from 39% to 87% (Fig. **F8**).

Recovery of Unit V (siliciclastic/volcaniclastic turbidite facies) was relatively good at Site C0012. The lithology consists of silicic tuff, volcaniclastic sandstone, siliciclastic sandstone, and hemipelagic mudstone (Fig. **F7**). There is a significant unconformity near the base of the unit, and the maximum age is >18.9 Ma. Mudstone interbeds within Unit V contain between 38% and 97% smectite in the clay-size fraction (average = 74%). Illite content averages 18%, chlorite + kaolinite averages 3%, and quartz averages 5%. This facies includes 11 identifiable bentonites, and Figure **F8** shows that smectite abundance in bulk mudstone ranges from 24% to 82% (average = 50%).

Unit IV is ~10 m thick and consists of reddish brown pelagic claystone with high concentrations of calcium carbonate. Samples from that unit were not analyzed for their clay-size mineral assemblages. Igneous basement (basalt) was also omitted from our XRD study, but information on its composition and alteration can be found in Kameda et al. (2011).

Figure **F9** demonstrates that the expandability of I/S mixed-layer clay minerals does not change significantly from the top of Unit I to the base of Unit V. The proportion of illite in the I/S averages 12% and ranges from 3% to 48%. The highest values of illite occur near the base of the sedimentary section, but there is no consistent pattern of progressive smectite-to-illite diagenesis as a function of depth. The estimated temperature at the top of basement is ~65°C (Expedition 333 Scientists, 2011). Values of illite crystallinity index typically range between 0.42 and 0.25 $\Delta°2\theta$, which is similar to what was detected at Site C0011. When compared to Site C0011, however, the results from Site C0012 display more scatter in illite crystallinity and a larger number of values fall within the diagenetic zone. This is likewise consistent with erosion of the illite as a detrital constituent from sedimentary source terrains that had been exposed to anchizone conditions of incipient metamorphism (e.g., Blenkinsop, 1988; Kisch, 1990).

Acknowledgments

This research used samples provided by the Integrated Ocean Drilling Program (IODP). We thank Captains Yasushi Minoura and Yuji Onda, as well as the Mantle Quest Japan drilling crew, Marine Works Japan laboratory technicians, and fellow scientists aboard the D/V *Chikyu* for their dedicated assistance during IODP Expedition 322. Funding was granted by the Consortium for Ocean Leadership, U.S. Science Support Program (Grants T315B58 and T322A58 to M.B. Underwood and Grant T315C58 to J. Guo), and the National Science Foundation (Grant OCE-07518190). U. Shriniwar assisted with sample preparation.

References

Ashi, J., Lallemant, S., Masago, H., and the Expedition 315 Scientists, 2009. Expedition 315 summary. *In* Kinoshita, M., Tobin, H., Ashi, J., Kimura, G., Lallemant, S., Screaton, E.J., Curewitz, D., Masago, H., Moe, K.T., and the Expedition 314/315/316 Scientists, *Proc. IODP,* 314/315/

316: Washington, DC (Integrated Ocean Drilling Program Management International, Inc.). **doi:10.2204/iodp.proc.314315316.121.2009**

Biscaye, P.E., 1964. Distinction between kaolinite and chlorite in recent sediments by X-ray diffraction. *Am. Miner.,* 49:1281–1289.

Biscaye, P.E., 1965. Mineralogy and sedimentation of recent deep-sea clay in the Atlantic Ocean and adjacent seas and oceans. *Geol. Soc. Am. Bull.,* 76(7):803–831. **doi:10.1130/0016-7606(1965)76[803:MASORD]2.0.CO;2**

Blenkinsop, T.G., 1988. Definition of low-grade metamorphic zones using illite crystallinity. *J. Metamorph. Geol.,* 6(5):623–636. **doi:10.1111/j.1525-1314.1988.tb00444.x**

Chamley, H., 1980. Clay sedimentation and paleoenvironment in the area of Daito Ridge (Northwest Philippine Sea) since the early Eocene. *In* Klein, G. de V., Kobayashi, K., et al., *Init. Repts. DSDP,* 58: Washington, DC (U.S. Govt. Printing Office), 683–693. **doi:10.2973/dsdp.proc.58.119.1980**

Chamley, H., Cadet, J.-P., and Charvet, J., 1986. Nankai Trough and Japan Trench late Cenozoic paleoenvironments deduced from clay mineralogic data. *In* Kagami, H., Karig, D.E., Coulbourn, W.T., et al., *Init. Repts. DSDP,* 87: Washington, DC (U.S. Govt. Printing Office), 633–641. **doi:10.2973/dsdp.proc.87.113.1986**

Cook, H.E., Zemmels, I., and Matti, J.C., 1975. X-ray mineralogy data, far western Pacific, Leg 31 Deep Sea Drilling Project. *In* Karig, D.E., Ingle, J.C., Jr., et al., *Init. Repts. DSDP,* 31: Washington (U.S. Govt. Printing Office), 883–895. **doi:10.2973/dsdp.proc.31.app.1975**

Expedition 322 Scientists, 2010a. Site C0011. *In* Saito, S., Underwood, M.B., Kubo, Y., and the Expedition 322 Scientists, *Proc. IODP,* 322: Tokyo (Integrated Ocean Drilling Program Management International, Inc.). **doi:10.2204/iodp.proc.322.103.2010**

Expedition 322 Scientists, 2010b. Site C0012. *In* Saito, S., Underwood, M.B., Kubo, Y., and the Expedition 322 Scientists, *Proc. IODP,* 322: Tokyo (Integrated Ocean Drilling Program Management International, Inc.). **doi:10.2204/iodp.proc.322.104.2010**

Expedition 333 Scientists, 2011. NanTroSEIZE Stage 2: subduction inputs 2 and heat flow. *IODP Prel. Rept.,* 333. **doi:10.2204/iodp.pr.333.2011**

Fagel, N., André, L., Chamley, H., Debrabant, P., and Jolivet, L., 1992. Clay sedimentation in the Japan Sea since the early Miocene: influence of source-rock and hydrothermal activity. *Sediment. Geol.,* 80(1–):27–40. **doi:10.1016/0037-0738(92)90029-Q**

Guo, J., and Underwood, M.B., 2011. Data report: refined method for calculating percentages of kaolinite and chlorite from X-ray diffraction data, with application to the Nankai margin of southwest Japan. *In* Kinoshita, M., Tobin, H., Ashi, J., Kimura, G., Lallemant, S., Screaton, E.J., Curewitz, D., Masago, H., Moe, K.T., and the Expedition 314/315/316 Scientists, *Proc. IODP,* 314/315/316: Washington, DC (Integrated Ocean Drilling Program Management International, Inc.). **doi:10.2204/iodp.proc.314315316.201.2011**

Guo, J., and Underwood, M.B., 2012. Data report: clay mineral assemblages from the Nankai Trough accretionary prism and the Kumano Basin, IODP Expeditions 315 and 316, NanTroSEIZE Stage 1. *In* Kinoshita, M., Tobin, H., Ashi, J., Kimura, G., Lallemant, S., Screaton, E.J., Curewitz, D., Masago, H., Moe, K.T., and the Expedition 314/315/316 Scientists, *Proc. IODP,* 314/315/316: Washington, DC (Integrated Ocean Drilling Program Management International, Inc.). **doi:10.2204/iodp.proc.314315316.202.2012**

Heath, G.R., and Pisias, N.G., 1979. A method for the quantitative estimation of clay minerals in North Pacific deep-sea sediments. *Clays Clay Miner.,* 27(3):175–184. **doi:10.1346/CCMN.1979.0270302**

Ike, T., Moore, G.F., Kuramoto, S., Park, J.-O., Kaneda, Y., and Taira, A., 2008. Tectonics and sedimentation around Kashinosaki Knoll: a subducting basement high in the eastern Nankai Trough. *Isl. Arc,* 17(3):358–375. **doi:10.1111/j.1440-1738.2008.00625.x**

Johnson, L.J., Chu, C.H., and Hussey, G.A., 1985. Quantitative clay mineral analysis using simultaneous linear equations. *Clays Clay Miner.,* 33(2):107–117. **doi:10.1346/CCMN.1985.0330204**

Kagami, H., Karig, D.E., Coulbourn, W.T., et al., 1986. *Init. Repts. DSDP,* 87: Washington, DC (U.S. Govt. Printing Office). **doi:10.2973/dsdp.proc.87.1986**

Kameda, J., Yamaguchi, A., Saito, S., Sakuma, H., Kawamura, K., and Kimura, G., 2011. A new source of water in seismogenic subduction zones. *Geophys. Res. Lett.,* 38(22):L22306. **doi:10.1029/2011GL048883**

Karig, D.E., Ingle, J.C., Jr., et al., 1975. *Init. Repts. DSDP,* 31: Washington, DC (U.S. Govt. Printing Office). **doi:10.2973/dsdp.proc.31.1975**

Kisch, H.J., 1990. Calibration of the anchizone: a critical comparison of illite "crystallinity" scales used for definition. *J. Metamorph. Geol.,* 8(1):31–46. **doi:10.1111/j.1525-1314.1990.tb00455.x**

Masuda, H., O'Neil, J.R., Jiang, W.-T., and Peacor, D.R., 1996. Relation between interlayer composition of authigenic smectite, mineral assemblages, I/S reaction rate and fluid composition in silicic ash of the Nankai Trough. *Clays Clay Miner.,* 44(4):443–459. **doi:10.1346/CCMN.1996.0440402**

Masuda, H., Peacor, D.R., and Dong, H., 2001. Transmission electron microscopy study of conversion of smectite to illite in mudstones of the Nankai Trough: contrast with coeval bentonites. *Clays Clay Miner.,* 49(2):109–118. **doi:10.1346/CCMN.2001.0490201**

McManus, D.A., 1991. Suggestions for authors whose manuscripts include quantitative clay mineral analysis by X-ray diffraction. *Mar. Geol.,* 98(1):1–5. **doi:10.1016/0025-3227(91)90030-8**

Moore, C.A., 1968. Quantitative analysis of naturally occurring multicomponent mineral systems by X-ray diffraction. *Clays Clay Miner.,* 16:325–336. **doi:10.1346/CCMN.1968.0160502**

Moore, D.M., and Reynolds, R.C., Jr., 1989. *X-Ray Diffraction and the Identification and Analysis of Clay Minerals:* Oxford (Oxford Univ. Press).

Moore, G.F., Mikada, H., Moore, J.C., Becker, K., and Taira, A., 2005. Legs 190 and 196 synthesis: deformation and fluid flow processes in the Nankai Trough accretionary prism. *In* Mikada, H., Moore, G.F., Taira, A., Becker, K., Moore, J.C., and Klaus, A. (Eds.), *Proc. ODP, Sci. Results,* 190/196: College Station, TX (Ocean Drilling Program), 1–25. **doi:10.2973/odp.proc.sr.190196.201.2005**

Moore, G.F., Taira, A., Klaus, A., Becker, L., Boeckel, B., Cragg, B.A., Dean, A., Fergusson, C.L., Henry, P., Hirano, S., Hisamitsu, T., Hunze, S., Kastner, M., Maltman, A.J., Morgan, J.K., Murakami, Y., Saffer, D.M., Sánchez-Gómez, M., Screaton, E.J., Smith, D.C., Spivack, A.J., Steurer, J., Tobin, H.J., Ujiie, K., Underwood, M.B., and Wilson, M., 2001. New insights into deformation and fluid flow processes in the Nankai Trough accretionary prism: results of Ocean Drilling Program Leg 190. *Geochem., Geophys., Geosyst.,* 2(10):1058. **doi:10.1029/2001GC000166**

Omotoso, O., McCarty, D.K., Hillier, S., and Kleeberg, R., 2006. Some successful approaches to quantitative mineral analysis as revealed by the 3rd Reynolds Cup contest. *Clays Clay Miner.,* 54(6):748–760. **doi:10.1346/CCMN.2006.0540609**

Ottner, F., Gier, S., Kuderna, M., and Schwaighofer, B., 2000. Results of an inter-laboratory comparison of methods for quantitative clay analysis. *Appl. Clay Sci.,* 17(5–6): 223–243. **doi:10.1016/S0169-1317(00)00015-6**

Rettke, R.C., 1981. Probable burial diagenetic and provenance effects on Dakota Group clay mineralogy, Denver Basin. *J. Sediment. Petrol.,* 51(2):541–551. **doi:10.1306/212F7CCF-2B24-11D7-8648000102C1865D**

Saffer, D.M., Underwood, M.B., and McKiernan, A.W., 2008. Evaluation of factors controlling smectite transformation and fluid production in subduction zones: application to the Nankai Trough. *Isl. Arc,* 17(2):208–230. **doi:10.1111/j.1440-1738.2008.00614.x**

Screaton, E.J., Kimura, G., Curewitz, D., and the Expedition 316 Scientists, 2009. Expedition 316 summary. *In* Kinoshita, M., Tobin, H., Ashi, J., Kimura, G., Lallemant, S., Screaton, E.J., Curewitz, D., Masago, H., Moe, K.T., and the Expedition 314/315/316 Scientists, *Proc. IODP,* 314/315/316: Washington, DC (Integrated Ocean Drilling Program Management International, Inc.). **doi:10.2204/iodp.proc.314315316.131.2009**

Spinelli, G.A., and Underwood, M.B., 2005. Modeling thermal history of subducting crust in Nankai Trough: constraints from in situ sediment temperature and diagenetic reaction progress. *Geophys. Res. Lett.,* 32(9):L09301. **doi:10.1029/2005GL022793**

Środoń, J., Drits, V.A., McCarty, D.K., Hsieh, J.C.C., and Eberl, D.D., 2001. Quantitative X-ray diffraction analysis of clay-bearing rocks from random preparations. *Clays Clay Miner.,* 49(6):514–528. **http://ccm.geoscienceworld.org/cgi/content/abstract/49/6/514**

Steurer, J.F., and Underwood, M.B., 2003. Clay mineralogy of mudstones from the Nankai Trough reference Sites 1173 and 1177 and frontal accretionary prism Site 1174. *In* Mikada, H., Moore, G.F., Taira, A., Becker, K., Moore, J.C., and Klaus, A. (Eds.), *Proc. ODP, Sci. Results,* 190/196: College Station, TX (Ocean Drilling Program), 1–37. **doi:10.2973/odp.proc.sr.190196.211.2003**

Taira, A., Hill, I., Firth, J., Berner, U., Brückmann, W., Byrne, T., Chabernaud, T., Fisher, A., Foucher, J.-P., Gamo, T., Gieskes, J., Hyndman, R., Karig, D., Kastner, M., Kato, Y., Lallemant, S., Lu, R., Maltman, A., Moore, G., Moran, K., Olaffson, G., Owens, W., Pickering, K., Siena, F., Taylor, E., Underwood, M., Wilkinson, C., Yamano, M., and Zhang, J., 1992. Sediment deformation and hydrogeology of the Nankai Trough accretionary prism: synthesis of shipboard results of ODP Leg 131. *Earth Planet. Sci. Lett.,* 109(3–4):431–450. **doi:10.1016/0012-821X(92)90104-4**

Tobin, H., Kinoshita, M., Ashi, J., Lallemant, S., Kimura, G., Screaton, E.J., Moe, K.T., Masago, H., Curewitz, D., and the Expedition 314/315/316 Scientists, 2009. NanTroSEIZE Stage 1 expeditions: introduction and synthesis of key results. *In* Kinoshita, M., Tobin, H., Ashi, J., Kimura, G., Lallemant, S., Screaton, E.J., Curewitz, D., Masago, H., Moe, K.T., and the Expedition 314/315/316 Scientists, *Proc. IODP,* 314/315/316: Washington, DC (Integrated Ocean Drilling Program Management International, Inc.). **doi:10.2204/iodp.proc.314315316.101.2009**

Underwood, M., Basu, N., Steurer, J., and Udas, S., 2003. Data report: normalization factors for semiquantitative X-ray diffraction analysis, with application to DSDP Site 297, Shikoku Basin. *In* Mikada, H., Moore, G.F., Taira, A., Becker, K., Moore, J.C., and Klaus, A. (Eds.), *Proc. ODP, Sci. Results,* 190/196: College Station, TX (Ocean Drilling Program), 1–28. **doi:10.2973/odp.proc.sr.190196.203.2003**

Underwood, M.B., 2007. Sediment inputs to subduction zones: why lithostratigraphy and clay mineralogy matter. *In* Dixon, T., and Moore, J.C. (Eds.), *The Seismogenic Zone of Subduction Thrust Faults:* New York (Columbia Univ. Press), 42–85.

Underwood, M.B., Orr, R., Pickering, K., and Taira, A., 1993a. Provenance and dispersal patterns of sediments in the turbidite wedge of Nankai Trough. *In* Hill, I.A., Taira, A., Firth, J.V., et al., *Proc. ODP, Sci. Results,* 131: College Station, TX (Ocean Drilling Program), 15–34. **doi:10.2973/odp.proc.sr.131.105.1993**

Underwood, M.B., and Pickering, K.T., 1996. Clay-mineral provenance, sediment dispersal patterns, and mudrock diagenesis in the Nankai accretionary prism, southwest Japan. *Clays Clay Miner.,* 44(3):339–356. **doi:10.1346/CCMN.1996.0440304**

Underwood, M.B., Pickering, K., Gieskes, J.M., Kastner, M., and Orr, R., 1993b. Sediment geochemistry, clay mineralogy, and diagenesis: a synthesis of data from Leg 131, Nankai Trough. *In* Hill, I.A., Taira, A., Firth, J.V., et al., *Proc. ODP, Sci. Results,* 131: College Station, TX (Ocean Drilling Program), 343–363. **doi:10.2973/odp.proc.sr.131.137.1993**

Underwood, M.B., Saito, S., Kubo, Y., and the Expedition 322 Scientists, 2010. Expedition 322 summary. *In* Saito, S., Underwood, M.B., Kubo, Y., and the Expedition 322

Scientists, *Proc. IODP,* 322: Tokyo (Integrated Ocean Drilling Program Management International, Inc.). **doi:10.2204/iodp.proc.322.101.2010**

Underwood, M.B., and Steurer, J.F., 2003. Composition and sources of clay from the trench slope and shallow accretionary prism of Nankai Trough. *In* Mikada, H., Moore, G.F., Taira, A., Becker, K., Moore, J.C., and Klaus, A. (Eds.), *Proc. ODP, Sci. Results,* 190/196: College Station, TX (Ocean Drilling Program), 1–28. **doi:10.2973/odp.proc.sr.190196.206.2003**

Initial receipt: 17 June 2011
Acceptance: 4 November 2012
Publication: 15 May 2013
MS 322-202

Figure F1. Map of the Nankai Trough and Shikoku Basin study area with IODP NanTroSEIZE drill site locations. Also shown are locations of DSDP and ODP transects and drill sites.

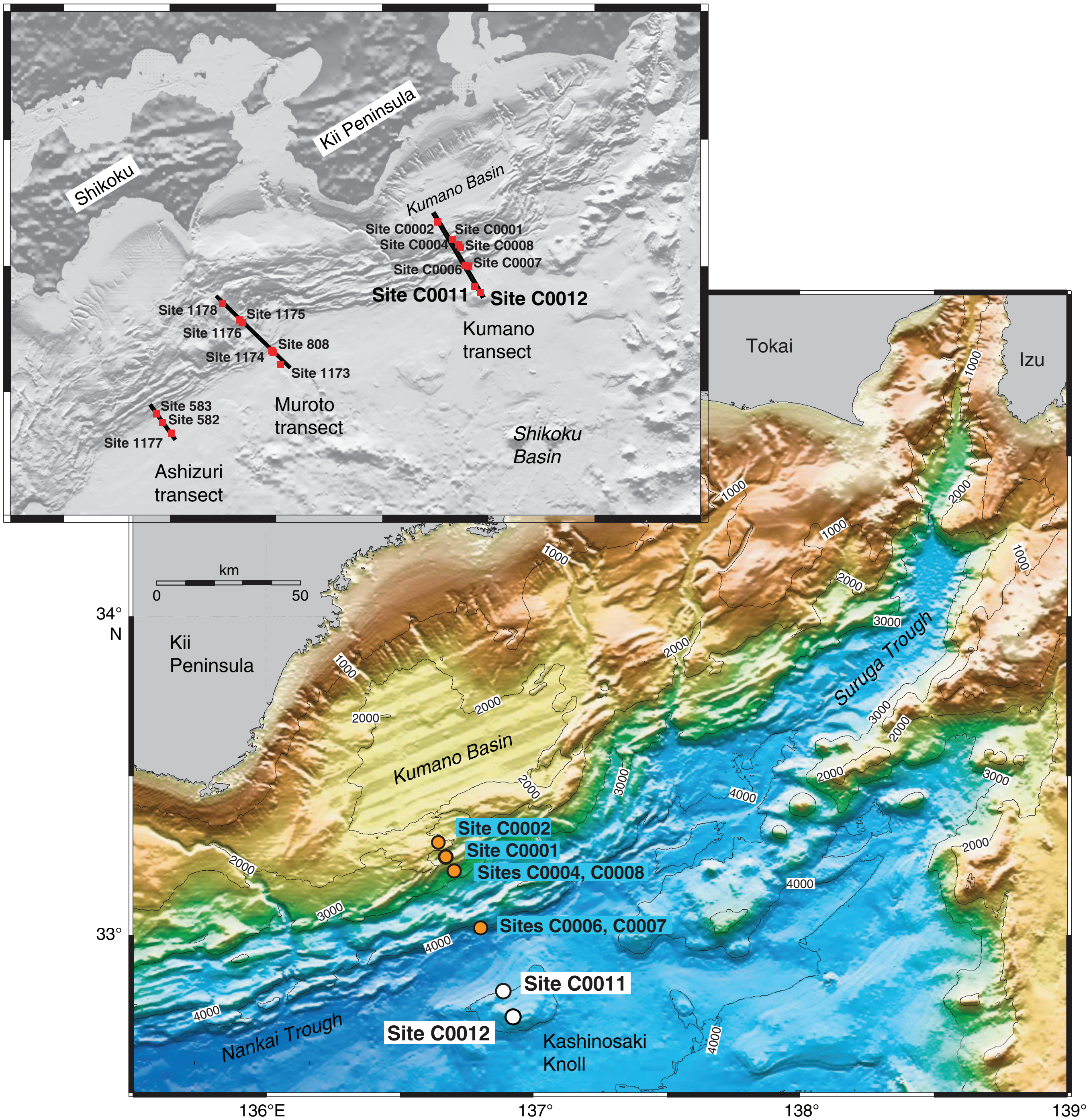

Figure F2. Seismic in-line section crossing the Kashinosaki Knoll showing locations of Sites C0011 and C0012 and interpretation of acoustic units based on core recovery. IFREE = Institute for Research on Earth Evolution. VE = vertical exaggeration.

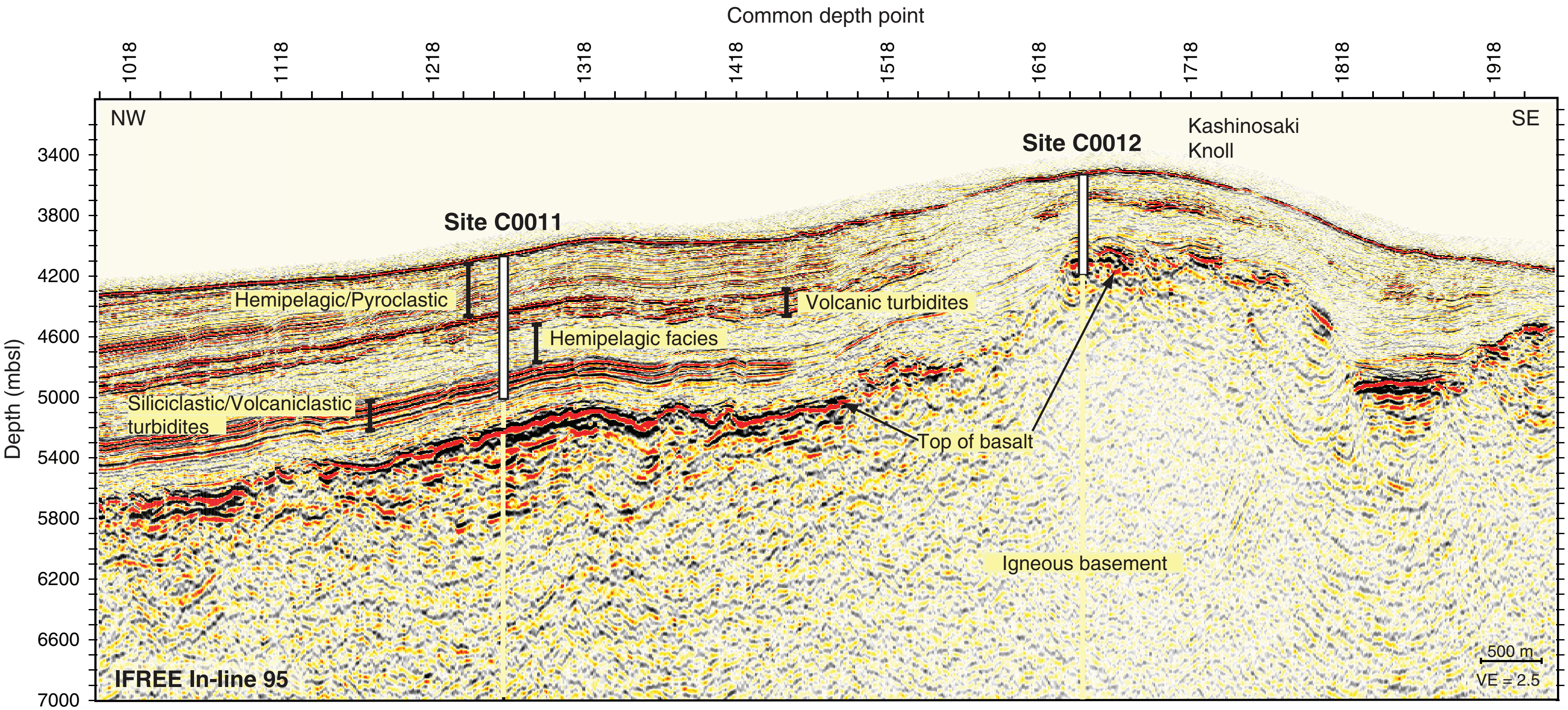

Figure F3. Representative examples of X-ray diffractograms showing peaks for smectite, illite, chlorite, kaolinite, and quartz, Sites C0011 and C0012. Values of relative mineral abundance (weight percent) were calculated using the SVD normalization factors of Underwood et al. (2003) and the following peak areas: smectite (001), illite (001), chlorite (002) + kaolinite (001), and quartz (100). Proportion of kaolinite to chlorite was calculated using the equations of Guo and Underwood (2011).

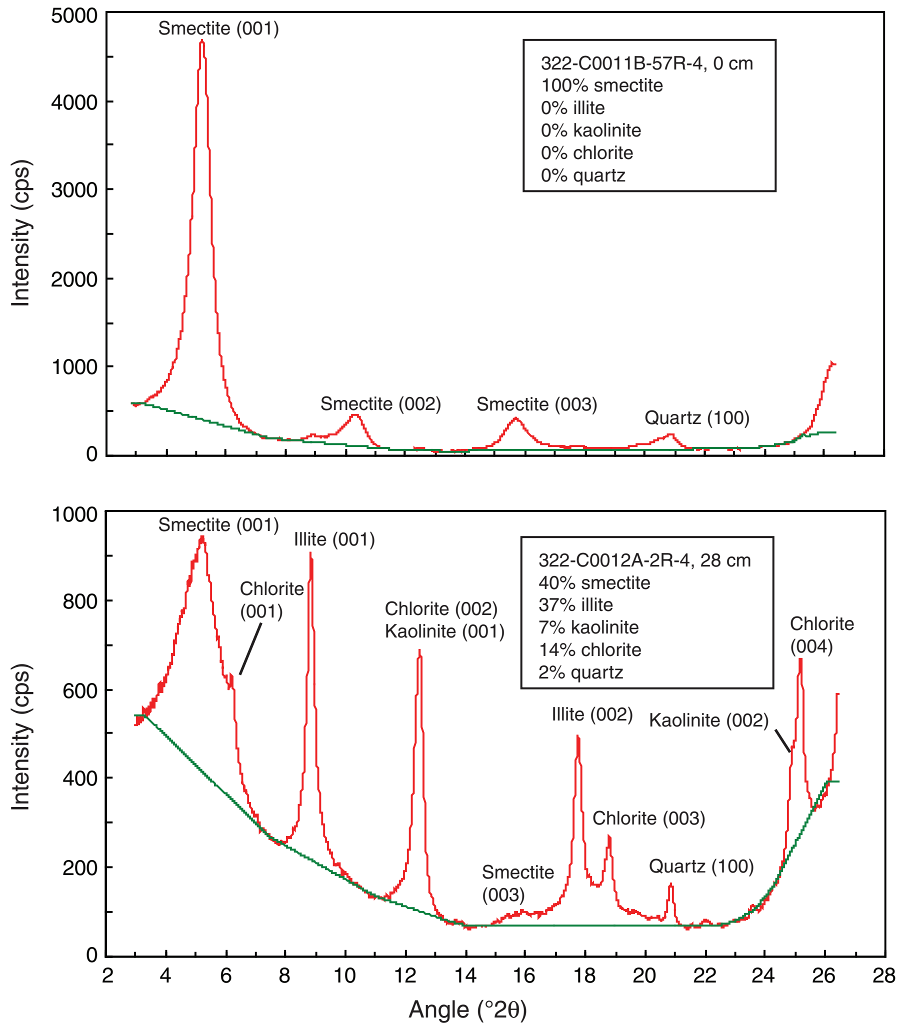

Figure F4. Lithostratigraphy of Site C0011 with relative abundances of smectite, illite, chlorite, kaolinite, and quartz in clay-size fractions of mud(stone). Ages at the boundaries are based on an integrated age-depth model (see the "Site C0011" chapter [Expedition 322 Scientists, 2010a]). Calculations were made using SVD normalization factors.

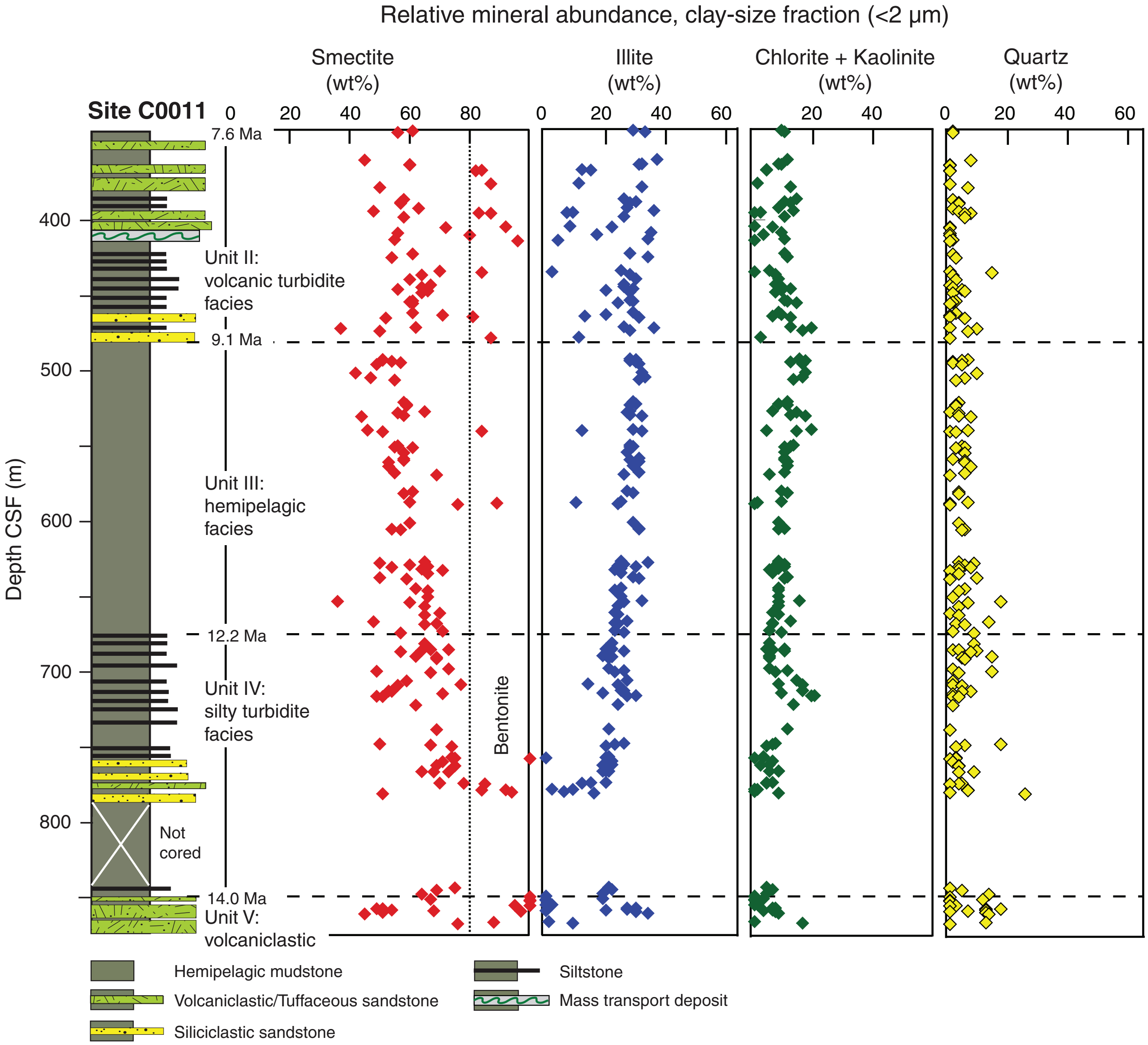

Figure F5. Lithostratigraphy of Site C0011 with relative abundances of total clay minerals in bulk mudstone relative to quartz + feldspar + calcite (see the **"Site C0011"** chapter [Expedition 322 Scientists, 2010a]), smectite in the clay mineral fraction (relative to illite + chlorite + kaolinite), and smectite in bulk mudstone. Calculations were made using SVD normalization factors.

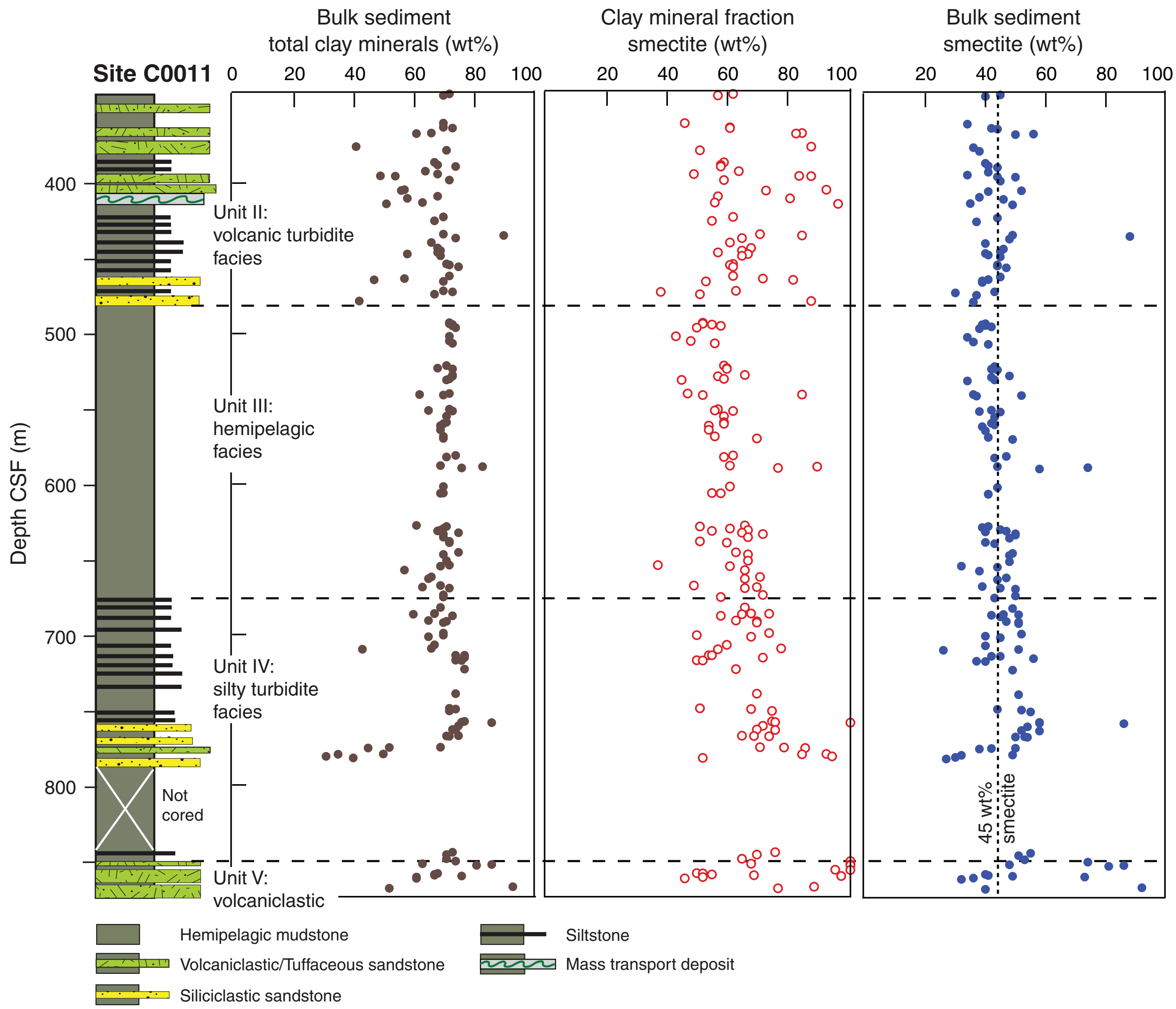

Figure F6. Lithostratigraphy of Site C0011 with values of illite/smectite (I/S) mixed-layer clay expandability, proportion of illite in I/S mixed-layer clay, and illite crystallinity index.

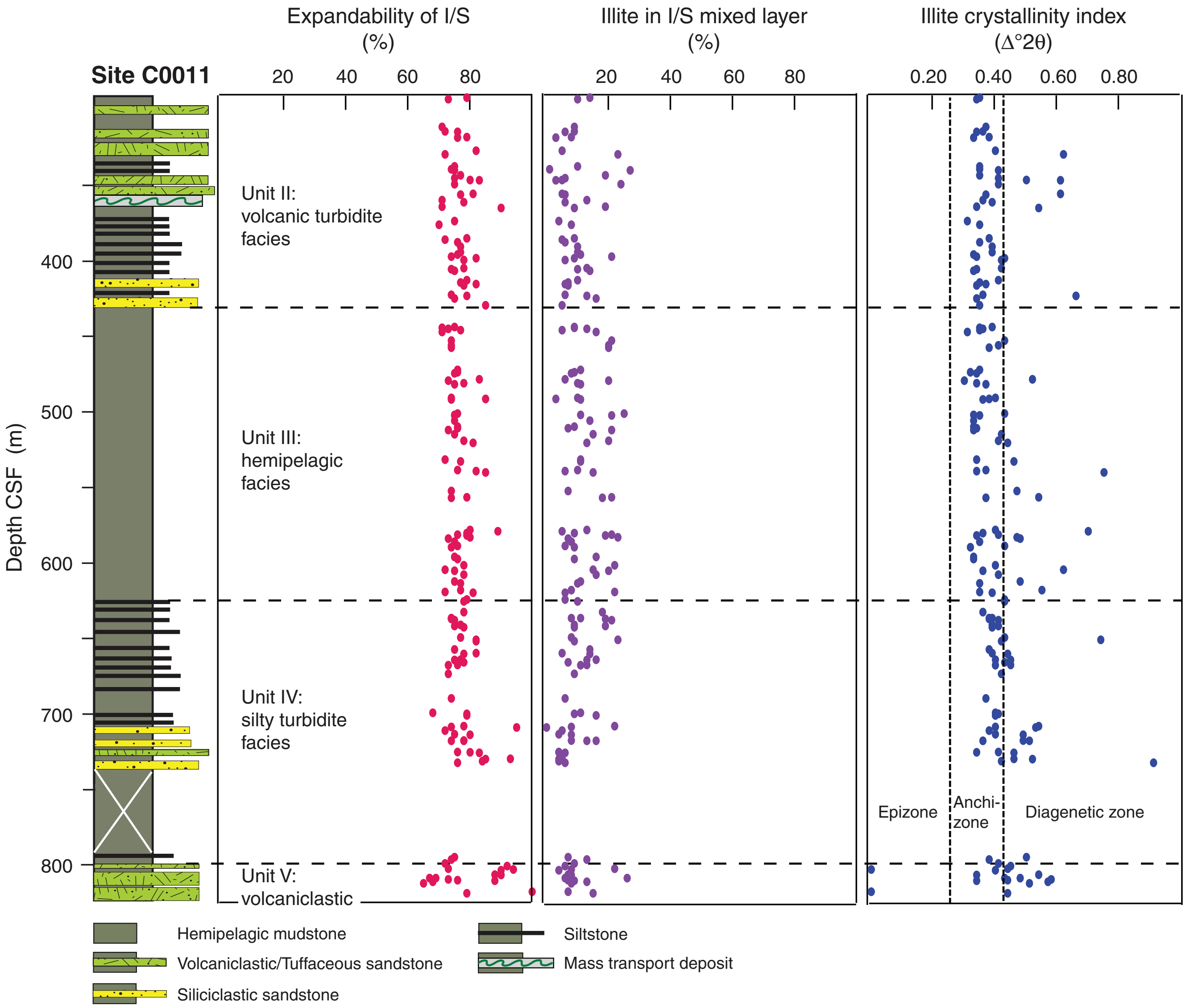

Figure F7. Lithostratigraphy of Site C0012 with relative abundances of smectite, illite, chlorite, kaolinite, and quartz in clay-size fractions of mud(stone). Ages at unit boundaries are based on an integrated age-depth model (see the **"Site C0012"** chapter [Expedition 322 Scientists, 2010b]). Calculations were made using SVD normalization factors.

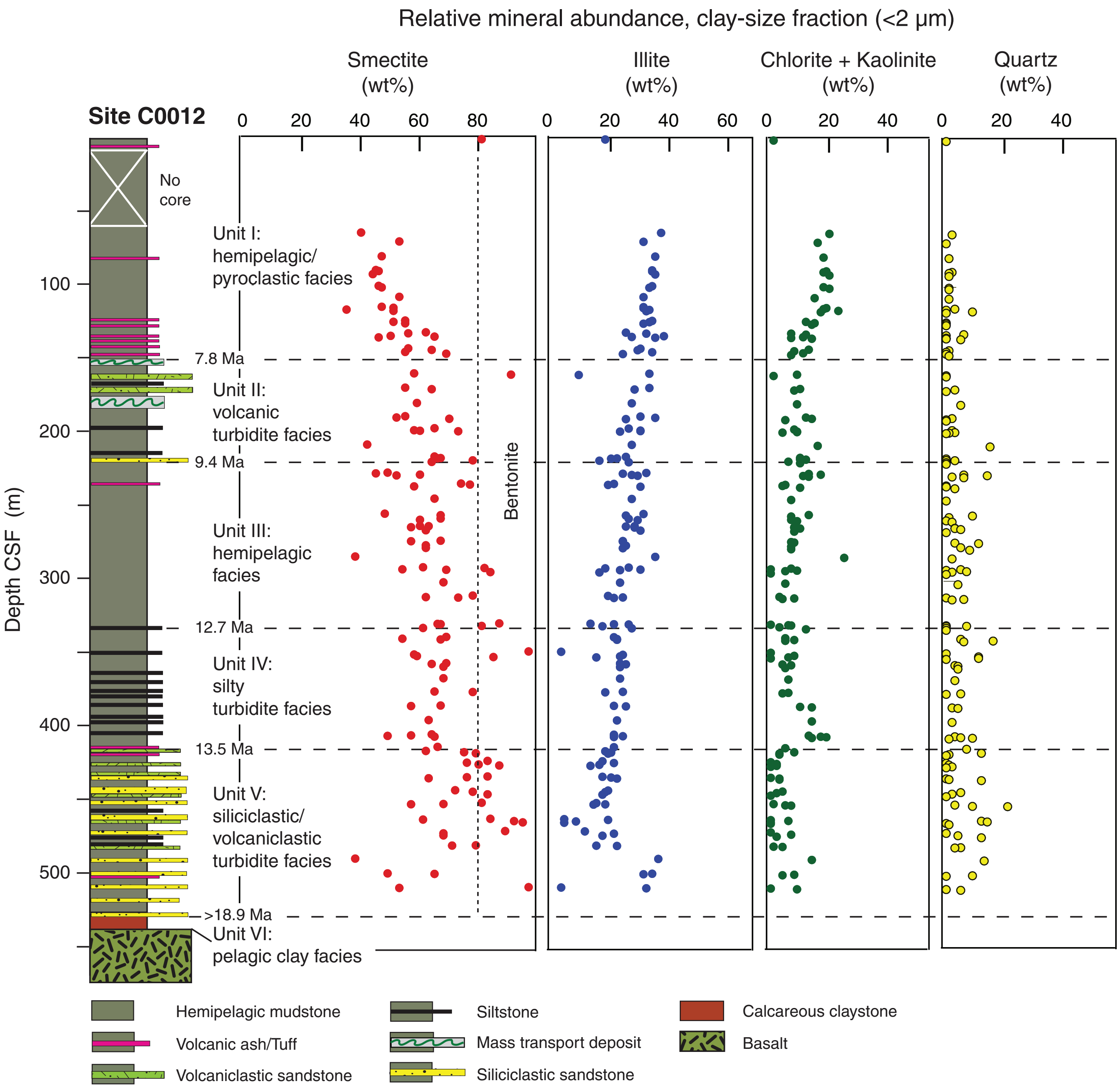

Figure F8. Lithostratigraphy of Site C0012 with relative abundances of total clay minerals in bulk mudstone relative to quartz + feldspar + calcite (see the **"Site C0012"** chapter [Expedition 322 Scientists, 2010b]), smectite in the clay mineral fraction (relative to illite + chlorite + kaolinite), and smectite in bulk mudstone. Calculations were made using SVD normalization factors.

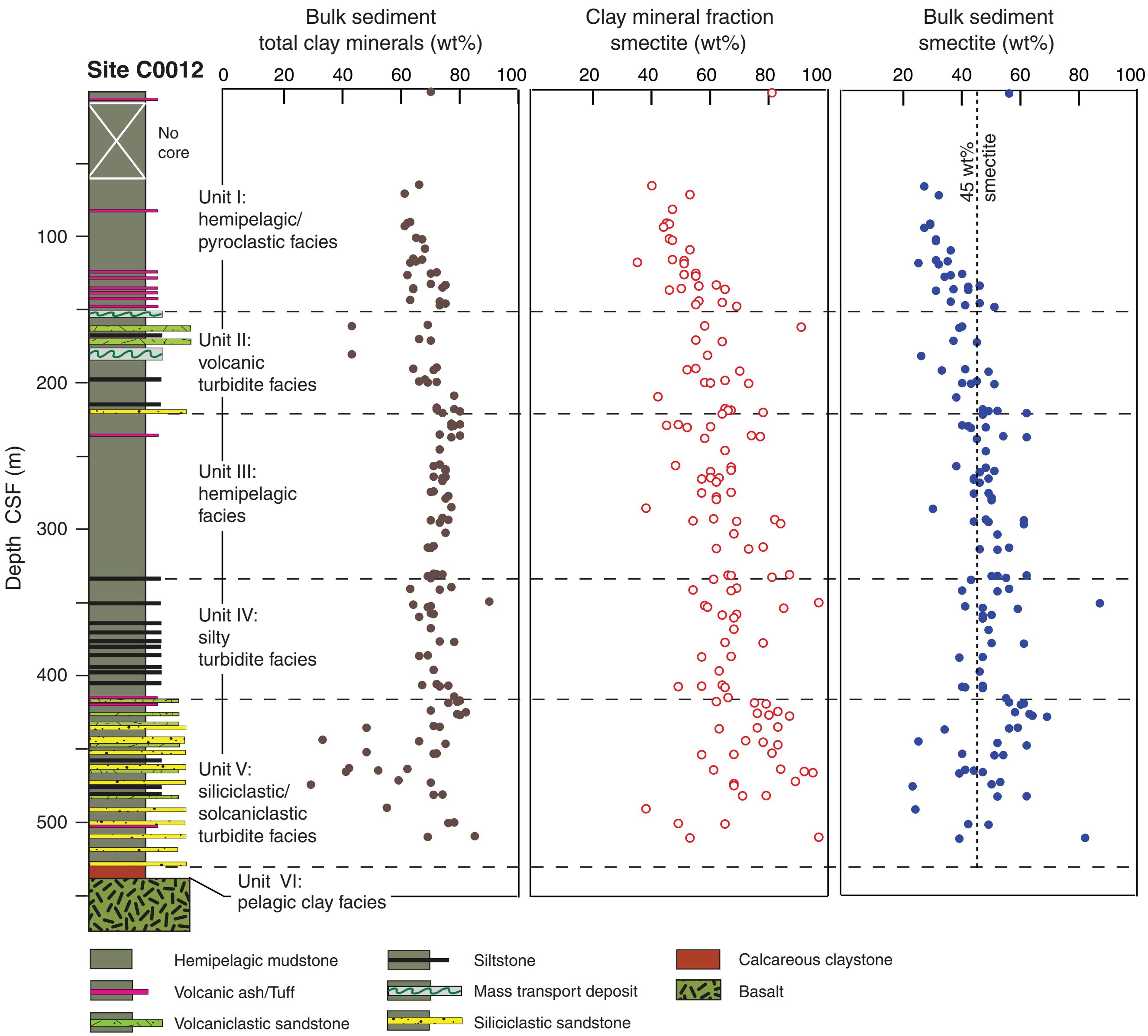

Figure F9. Lithostratigraphy of Site C0012 with values of illite/smectite (I/S) mixed-layer clay expandability, proportion of illite in I/S mixed-layer clay, and illite crystallinity index.

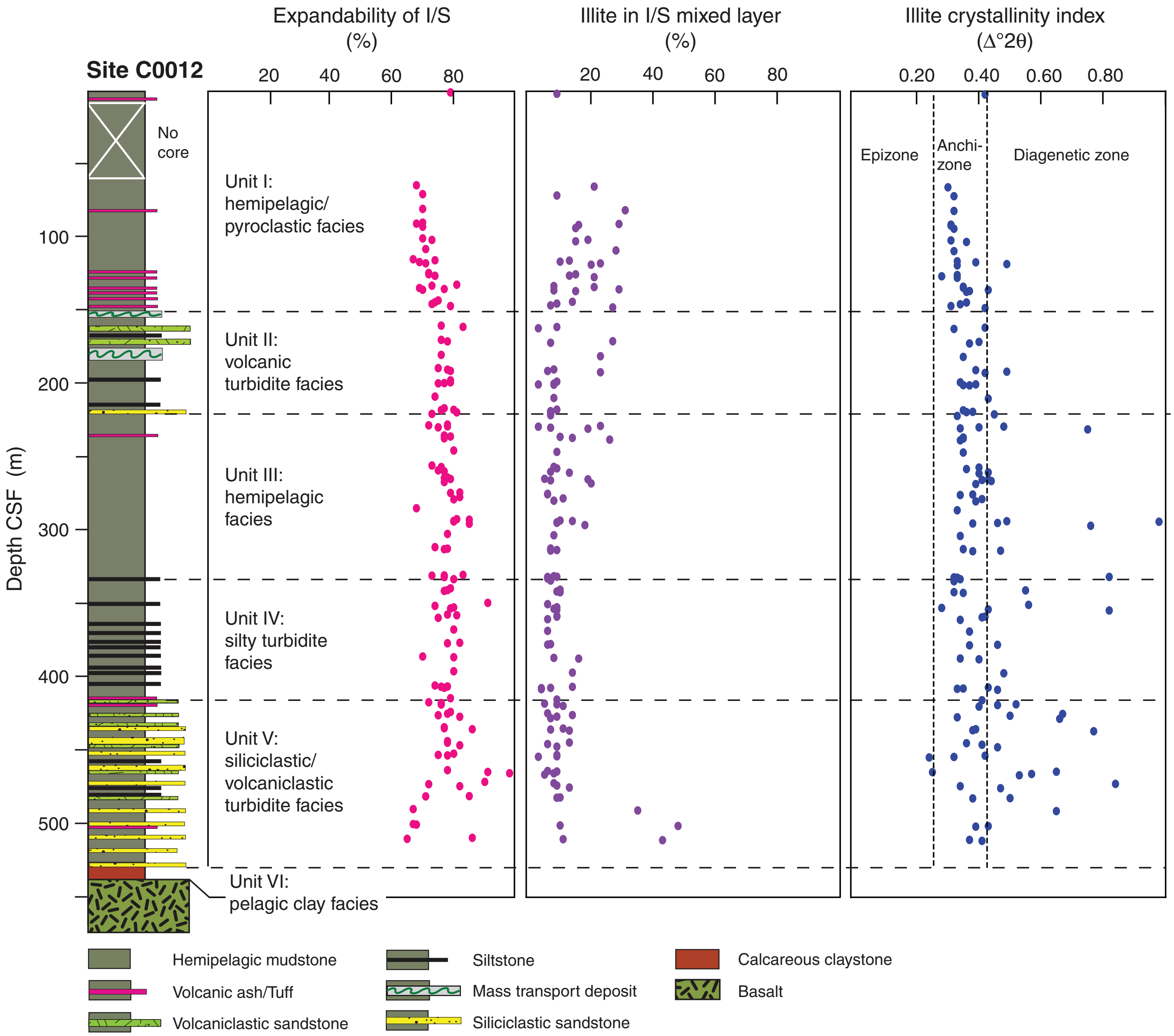

Table T1. Singular value decomposition normalization factors (from Underwood et al., 2003) used to calculate relative mineral abundances in clay-size aggregates (<2 µm size fraction).

<2 µm fraction	Affected mineral standard mixture			
	Smectite	Illite	Chlorite	Quartz
Influencing mineral:				
Smectite	3.7398559E–04	–2.8994615E–05	–3.4377535E–05	–7.4421238E–05
Illite	4.2720105E–05	1.2499784E–03	–2.836388E–05	3.3838456E–05
Chlorite	–6.7662186E–05	–2.008419E–07	7.6974847E–04	5.240881E–05
Quartz	2.4368789E–03	9.2311541E–04	8.195109E–04	3.7061975E–03

Table T2. Results of X-ray diffraction analysis (<2 µm size fraction) with values of peak area for diagnostic clay mineral reflections, Sites C0011 and C0012. (Continued on next four pages.)

Core, section, interval (cm)	Depth CSF (m)	Integrated peak area (total counts)					
		Smectite (001)	Illite (001)	Chlorite (002) + kaolinite (001)	Quartz (100)	Half peak chlorite (004)	Kaolinite (002) + chlorite (004)
322-C0011B-							
Unit II - volcanic turbidite facies							
1R-1, 41	340.41	136,258	23,104	14,834	2,537	5,078	12,192
1R-2, 25	341.43	149,460	31,291	19,049	2,651	5,996	13,214
3R-2, 25	359.86	57,856	17,322	9,763	1,954	2,903	7,183
3R-4, 118	362.73	136,198	25,327	14,169	2,021	4,533	9,551
3R-5, 18	363.15	140,765	25,292	15,888	1,867	4,480	10,409
4R-2, 45	366.66	153,011	9,395	8,632	1,822	2,229	5,228
4R-3, 0	366.94	177,489	13,178	10,654	1,632	2,818	7,143
5R-2, 25	375.62	211,631	12,289	9,754	1,814	2,016	4,961
5R-4, 105	378.02	53,045	12,318	8,744	1,582	1,705	6,524
6R-2, 70	386.11	134,923	21,574	21,633	2,533	6,681	16,525
6R-3, 105	387.87	154,290	28,438	19,449	3,340	4,823	13,033
6R-5, 25	388.68	150,197	25,816	20,996	3,452	6,278	16,125
6R-8, 15	391.92	112,014	17,360	11,040	2,226	3,186	7,727
7R-1, 38	393.88	46,684	12,257	8,207	1,012	1,926	4,885
7R-2, 7	394.98	56,039	2,198	1,528	1,609		
7R-3, 0	395.14	83,140	2,548	1,622	2,237	316	912
7R-5, 101	397.85	93,895	15,176	11,082	2,588	3,794	7,872
8R-2, 0	404.27	81,732	3,022	2,120	1,604		
8R-3, 19	404.78	122,136	13,909	9,036	2,243	3,328	7,124
8R-5, 104	408.50	143,985	31,242	17,596	2,378	4,919	11,628
8R-6, 107	409.89	164,496	14,094	9,325	1,683	2,886	6,129
9R-1, 32	412.82	103,765	22,460	14,208	1,890	4,015	8,795
9R-2, 0	413.63	225,727	5,948	3,167	3,040	705	1,779
10R-1, 32	422.32	151,420	24,308	17,514	2,928	5,849	12,806
10R-3, 0	424.75	147,404	32,839	20,546	2,981	6,375	14,685
11R-2, 85	433.75	205,953	27,002	14,169	2,955	3,677	7,898
11R-4, 0	434.64	30,660	0	0	1,262		
11R-5, 107	436.31	145,830	23,009	13,265	2,684	4,192	8,438
11R-7, 132	439.38	137,253	24,550	14,437	2,804	4,876	10,084
12R-2, 50	442.91	157,383	21,901	13,625	2,636	3598	8,799
12R-3, 75	444.58	122,227	17,798	12,611	2,418	3,816	9,037
12R-4, 62	445.87	111,073	20,155	16,059	2,677	4,581	10,667
12R-6, 0	446.96	93,993	10,466	9,193	2,471	2,800	6,486
12R-7, 83	448.16	157,568	24,445	14,648	2,957	4,596	9,863
13R-3, 30	453.62	186,927	31,007	21,679	3,751	6,678	14,217
13R-4, 51	454.19	161,309	27,617	20,602	2,958	4,655	13,379
13R-5, 26	455.35	137,596	19,502	21,219	2,329	5,794	15,307
14R-2, 17	461.59	159,907	26,894	16,024	3,251	4,362	10,568
14R-4, 0	463.16	209,031	22,275	20,824	2,537	5,814	14,634
14R-5, 45	464.07	284,530	19,536	21,303	2,095	4,788	12,685
14R-6, 4	465.08	95,615	19,946	14,654	2,641	4,853	11,218
15R-2, 45	471.35	157,778	23,976	21,545	2,670	6,511	15,676
15R-3, 0	472.03	45,934	16,411	14,870	1,941	4,546	11,205
15R-4, 117	473.72	105,315	20,568	20,774	3,253	7,234	16,232
16R-2, 0	478.21	229,271	13,107	11,850	2,003	2,574	6,348
Unit III - hemipelagic facies							
19R-3, 0	492.65	104,634	20,212	19,219	3,230	5,337	12,948
19R-4, 20	493.22	122,039	25,145	22,538	3,025	6,576	15,987
19R-4, 74	493.76	150,365	26,900	30,489	2,684	9,456	22,181
19R-5, 32	494.72	190,021	35,119	27,913	3,317	6,554	19,069
19R-6, 19	495.95	122,930	26,989	25,607	2,944	7,522	16,830
21R-2, 0	501.65	74,157	20,806	19,103	2,919	5,970	16,032
21R-4, 106	504.73	100,187	24,704	21,519	2,770	7,414	16,786
21R-5, 130	506.38	158,601	31,101	24,641	3,150	6,795	16,012
23R-2, 0	521.15	152,220	26,916	19,859	3,321	5,618	13,881
23R-3, 117	522.74	112,432	20,374	12,054	2,351	3,515	8,362
23R-4, 30	523.27	156,212	26,249	21,155	3,136	6,058	15,230
23R-7, 106	527.36	291,309	45,019	25,512	3,148	6,598	14,471
23R-8, 53	528.24	126,261	21,876	20,571	2,741	5,952	14,156
24R-1, 0	529.90	157,909	27,014	22,541	3,403	6,266	16,363
24R-2, 17	530.64	89,972	23,266	21,353	3,051	6,318	15,314
25R-1, 30	539.70	97,848	22,048	24,858	3,020	8,572	18,970
25R-2, 50	540.36	243,820	14,770	13,781	3,115	3,669	9,326
25R-3, 22	540.71	136,222	30,230	24,849	2,802	7,317	18,377

Table T2 (continued). (Continued on next page.)

Core, section, interval (cm)	Depth CSF (m)	Integrated peak area (total counts)					
		Smectite (001)	Illite (001)	Chlorite (002) + kaolinite (001)	Quartz (100)	Half peak chlorite (004)	Kaolinite (002) + chlorite (004)
26R-1, 112	550.12	120,296	21,169	18,562	2,951	5,405	13,473
26R-2, 67	550.89	126,336	23,550	17,985	3,346	5,177	13,093
26R-3, 25	551.27	149,337	24,102	17,581	2,956	5,902	12,538
26R-5, 104	554.72	118,169	19,922	14,851	3,132	4,418	10,057
27R-1, 22	558.72	164,669	30,489	20,833	3,099	6,281	13,121
27R-2, 48	559.84	113,597	19,786	13,477	3,014	3,894	9,249
27R-3, 115	561.07	122,383	25,184	16,973	3,397	5,917	12,469
27R-5, 110	563.81	86,894	17,442	11,843	2,813	3,922	8,733
28R-1, 15	568.17	120,696	24,213	15,567	3,234	4,628	9,903
28R-2, 0	569.46	284,187	38,419	21,272	2,831	5,965	12,493
30R-1, 30	580.70	150,398	23,897	17,028	3,368	4,622	11,831
30R-2, 0	581.78	139,758	24,424	18,371	3,041	5,436	13,856
31R-1, 108	587.58	128,999	19,803	14,193	3,692	4,048	10,229
31R-2, 50	588.36	217,399	11,178	8,447	2,655	1,221	4,632
31R-3, 77	589.17	267,358	31,138	9,525	2,392	2,166	5,363
32R-5, 0	601.39	159,545	27,234	16,047	3,580	3,569	9,364
33R-1, 22	605.72	92,028	18,772	11,592	2,479	3,690	8,356
33R-2, 0	605.94	138,736	26,742	14,429	3,336	4,098	8,964
35R-3, 23	627.39	127,964	17,373	11,545	2,902	3,684	7,767
35R-4, 0	628.14	107,222	26,925	12,383	3,856	3,959	9,004
35R-5, 87	629.47	104,269	15,917	11,662	2,824	3,067	8,221
35R-6, 60	630.54	158,733	21,178	13,326	3,584	4,222	9,066
35R-6, 115	631.06	102,424	20,365	12,594	3,267	3,122	7,389
35R-7, 94	632.21	138,468	19,119	13,248	3,211	3,955	8,758
35R-8, 44	633.08	177,522	20,782	12,399	3,328	3,162	7,547
36R-2, 50	635.17	144,557	19,489	11,125	3,255	3,290	6,962
36R-4, 127	637.89	89,198	18,957	12,794	3,546	3,668	8,946
36R-5, 69	638.72	154,327	28,503	19,933	2,333	6,300	14,650
37R-2, 50	645.18	129,773	19,298	12,709	3,436	3,673	8,903
37R-4, 9	646.61	131,399	16,371	12,167	2,917	3,828	8,338
37R-7, 33	650.81	164,026	22,548	15,049	3,146	4,730	9,752
38R-1, 72	653.72	38,464	14,142	10,411	3,389	2,440	8,434
38R-2, 0	654.39	129,650	20,274	13,134	3,830	3,988	8,752
38R-4, 64	656.98	118,688	15,584	11,393	2,738	2,995	7,500
38R-7, 92	661.49	174,515	21,151	13,014	3,229	3,994	8,089
39R-1, 23	662.74	139,374	18,431	13,358	3,208	3,760	8,106
39R-4, 50	667.24	56,514	11,963	9,232	3,019	2,271	6,533
39R-5, 108	668.41	153,461	18,260	11,518	3,378	3,389	7,175
39R-6, 25	669.00	138,056	18,239	9,550	3,768	2,804	6,268
40R-2, 17	673.57	182,688	21,515	12,165	3,594	3,291	7,401
Unit IV - silty turbidite facies							
40R-3, 0	674.82	95,516	15,860	10,227	3,198	3,389	7,375
42R-2, 0	681.88	127,150	15,420	8,159	4,186	2,284	4,770
43R-2, 40	685.81	173,795	20,762	19,422	3,172	4,899	12,006
43R-3, 0	685.87	173,808	17,871	8,838	4,174	2,212	4,984
43R-4, 56	686.36	109,067	13,069	7,038	3,897	2,073	4,319
43R-5, 117	687.27	86,010	14,126	10,768	2,679	3,174	7,746
44R-2, 0	690.41	131,776	14,478	5,794	6,399	836	2,613
44R-3, 0	691.09	159,506	18,528	10,528	3,872	2,655	6,490
44R-4, 21	691.90	166,036	18,582	9,742	4,458	2,765	5,735
45R-1, 24	698.74	176,996	18,541	12,059	3,602	3,328	7,289
45R-3, 0	700.28	61,229	12,188	8,948	3,370	2,236	4,976
45R-4, 36	701.18	148,551	18,147	12,845	3,406	2,977	8,166
45R-8, 12	706.66	171,103	27,490	27,027	3,132	6,779	17,964
46R-1, 105	709.05	175,240	12,153	14,964	3,491	2,737	9,558
46R-2, 25	709.65	135,007	20,202	24,504	3,190	5,988	17,683
47R-3, 33	713.52	134,667	22,069	24,980	4,153	5,975	16,047
47R-3, 36	713.56	132,350	22,961	25,434	3,079	6,009	15,045
47R-4, 60	715.20	182,462	18,014	16,907	3,571	4,859	10,555
47R-5, 83	716.85	121,022	25,082	30,408	2,030	7,754	20,357
47R-5, 113	717.15	103,937	19,378	23,691	2,322	7,288	17,813
48R-3, 25	722.79	195,863	27,234	28,133	3,463	7,285	17,670
50R-2, 29	739.11	191,799	21,357	21,921	2,883	4,187	11,792
51R-1, 136	748.76	55,430	11,185	4,389	3,770	1,273	2,888
51R-2, 58	749.31	153482	18,885	11,023	4,064	3,021	6,849
51R-4, 0	750.51	182,608	18,037	10,873	3,834	2,622	5,981
52R-1, 60	757.56	182,357	18,741	9,204	3,903	1,980	5,499

Table T2 (continued). (Continued on next page.)

Core, section, interval (cm)	Depth CSF (m)	Integrated peak area (total counts)					
		Smectite (001)	Illite (001)	Chlorite (002) + kaolinite (001)	Quartz (100)	Half peak chlorite (004)	Kaolinite (002) + chlorite (004)
52R-1, 113	758.04	170,208	16,801	8,445	3,665	2,258	5,028
52R-2, 11	758.40	442,028	4,036	667	5,220		
52R-3, 95	760.49	152,839	17,248	11,407	3,106	3,016	6,667
52R-5, 82	763.00	165,790	19,629	11,378	3,855	2,715	6,787
52R-6, 0	763.34	249,449	22,836	10,190	6,010	1,385	4,591
53R-1, 82	767.05	94,371	10,788	8,008	3,102	2,103	4,588
53R-1, 112	767.24	173,086	19,003	15,294	4,090	3,768	8,331
53R-2, 0	767.30	165,949	16,188	10,435	3,831	2,716	6,217
54R-5, 44	774.68	164,097	16,781	11,527	4,213	2,505	7,326
54R-5, 70	774.94	186,251	13,220	10,024	4,397	1,736	5,712
54R-5, 110	775.34	243,252	13,711	12,486	4,286	1,995	7,096
55R-1, 27	779.27	289,506	3,304	1,111	7,894		
55R-2, 0	779.50	126,857	5,185	2,565	3,542		
55R-3, 77	780.87	257,409	8,142	4,842	4,602	786	2,424
55R-5, 23	781.85	35,552	3,746	2,189	3,619	378	1,105
56R-2, 0	844.53	183,721	18,917	11,465	3,114	3,110	6,461
56R-3, 100	846.03	154,206	17,892	10,779	3,703	2,471	5,761
57R-2, 96	848.77	102,815	10,529	3,979	4,754	971	2,611
Unit V - volcaniclastic facies							
57R-4, 0	850.45	387,711	3,859	860	6,071		
57R-5, 120	852.25	116,274	11,623	3,475	4,685	705	1,814
57R-6, 23	852.69	445,681	0	0	4,505		
57R-6, 74	853.20	339,607	1,393	11,679	3,238	1,616	4,417
58R-1, 21	856.11	144,835	2,266	4,184	3,166	700	1,870
58R-1, 48	856.38	133,031	969	638	2,710		
58R-2, 119	858.42	56,584	11,841	4,650	3,800	1,162	2,569
58R-3, 0	858.47	77,345	17,259	5,808	3,811	1,393	3,454
58R-4, 40	859.27	84,733	15,982	6,358	4,072	1,232	3,222
58R-4, 100	859.84	151,471	16,321	10,466	4,283	2,495	5,433
58R-5, 0	860.23	289,529	2,084	17,883	0	3,186	7,112
58R-5, 72	860.91	70,932	15,433	6,760	3,396	1,614	4,185
58R-6, 44	861.87	57,782	16,815	6,463	3,195	1,968	4,242
59R-3, 0	867.48	481,439	0	0	17,620		
59R-4, 45	868.44	142,510	7,050	19,827	1,882	4,587	11,419
322-C0012A-							
Unit I - hemipelagic/pyroclastic facies							
1R-1, 62	0.62	277,694	24,340	11,820	3,399	2,786	6,141
2R-4, 28	64.13	86,015	27,426	26,433	1,692	6,410	16,883
3R-1, 72	70.22	77,090	15,456	14,854	1,203	4,675	12,166
4R-2, 25	80.26	88,590	22,515	21,244	1,443	7,080	17,537
5R-2, 25	89.68	112,413	29,235	29,630	2,215	8,925	22,740
5R-3, 42	90.31	126,985	32,504	30,988	2,226	8,727	23,690
5R-5, 18	92.49	97,525	26,044	27,078	1,611	8,584	22,616
6R-3, 10	100.45	114,445	29,175	27,836	2,049	7,605	20,191
6R-4, 71	101.39	116,126	27,699	30,319	1,915	8,321	23,552
7R-5, 108	107.84	124,222	25,492	23,192	2,066	4,842	15,098
8R-3, 30	114.62	63,631	14,369	15,777	1,346	5,042	12,554
8R-3, 108	115.40	98,500	20,374	21,549	1,555	6,599	15,957
8R-5, 0	116.62	39,353	13,888	16,320	1,769	6,138	14,389
8R-6, 47	117.33	124,561	26,468	26,151	1,923	7,024	18,402
9R-4, 0	124.03	191,303	40,511	29,445	2,240	8,765	20,813
9R-5, 59	124.86	125,410	28,282	24,045	2,001	7,553	18,988
9R-6, 30	125.98	118,472	23,282	20,264	1,720	5,948	15,958
10R-2, 41	132.03	114,421	16,920	9,351	3,408	3,064	6,718
10R-3, 44.5	132.62	162,741	32,342	23,967	2,281	6,546	15,789
10R-5, 35	134.39	76,744	19,932	12,242	820	3,210	8,019
10R-5, 92	134.96	158,779	23,657	15,339	1,955	4,296	10,397
10R-6, 0	135.44	72,149	19,597	13,961	1,921	4,690	11,122
11R-3, 24	142.89	124,762	23,442	19,334	2,336	6,219	14,055
11R-4, 0	144.03	174,780	27,782	17,632	1,832	4,856	12,413
11R-5, 107	145.37	159,393	34,583	23,567	2,256	6,901	16,263
11R-6, 113	146.64	156,417	19,613	13,235	2,953	3,214	8,334
Unit II - volcanic turbidite facies							
13R-2, 25	159.89	147,867	29,476	17,178	2,457	4,930	10,983
13R-3, 68	160.81	175,224	7,900	6,668	2,090	1,633	3,795
14R-2, 0	169.69	125,658	26,806	16,025	2,764	5,308	11,426

Table T2 (continued). (Continued on next page.)

Core, section, interval (cm)	Depth CSF (m)	Integrated peak area (total counts)					
		Smectite (001)	Illite (001)	Chlorite (002) + kaolinite (001)	Quartz (100)	Half peak chlorite (004)	Kaolinite (002) + chlorite (004)
14R-3, 85	170.83	136,071	20,974	13,352	2,366	3,819	8,147
15R-3, 0	180.09	79,395	13,079	8,715	2,082	3,057	6,672
16R-3, 0	189.03	14,1986	27,404	21,190	2,959	6,518	15,901
16R-4, 68	189.99	10,7893	25,148	19,127	1,486	4,863	12,276
16R-5, 12	190.85	20,7329	27,281	14,944	2,518	4,126	11,269
17R-1, 28	197.28	15,5453	22,139	14,670	3,169	4,279	10,837
17R-2, 45	198.65	12,0449	22,224	13,095	2,774	4,038	8,550
17R-3, 27	199.09	15,7968	28,416	17,144	3,027	4,785	11,167
17R-4, 17	199.28	18,2100	21,090	12,036	2,369	2,558	7,303
18R-2, 48	208.38	37,879	9,334	9,354	2,517	2,185	8,167
19R-1, 79	216.49	228,186	31,673	25,593	3,510	6,975	16,871
19R-2, 51	217.56	249,898	30,258	28,166	3,716	7,351	18,725
19R-3, 12	217.70	144,555	15,642	17,762	3,176	5,044	12,849
19R-4, 17	219.15	260,181	20,289	17,970	4,497	4,666	11,352
Unit III - hemipelagic facies							
19R-4, 122	220.20	173,251	25,345	19,985	2,732	4,662	13,121
20R-3, 0	227.50	113,876	26,433	19,882	3,528	5,563	14,539
20R-4, 16	228.00	32,666	6,365	7,680	1,935	2,820	8,184
20R-4, 100	228.84	160,150	25,656	19,996	3,225	5,341	12,649
20R-5, 20	229.44	56,385	11,128	9,234	1,653	2,504	6,144
21R-1, 23	234.93	226,148	23,411	16,199	3,357	3,721	9,866
21R-2, 30	235.69	230,447	21,656	13,150	3,777	3,793	8,669
21R-3, 105	236.77	130,874	23,885	15,983	2,936	4,653	10,445
22R-1, 109	245.29	162,811	24,310	14,946	2,959	4,742	10,951
23R-2, 45	255.52	82,362	19,285	14,453	3,204	4,013	9,825
23R-3, 45	256.55	162,456	21,882	14,573	3,068	4,166	9,863
23R-5, 91	258.75	132,434	18,344	11,294	2,401	3,138	7,100
23R-6, 43	259.51	152,537	26,528	17,470	3,017	5,070	11,990
24R-1, 48	263.68	125,380	20,940	13,067	2,989	3,579	9,195
24R-2, 0	263.93	155,397	22,481	15,365	3,634	3,755	10,698
24R-3, 48	264.76	114,578	20,222	14,384	3,044	4,566	10,551
24R-4, 98	266.67	229,284	39,050	22,874	3,280	5,707	12,401
25R-1, 110	273.80	162,477	21,231	12,964	3,688	3,183	7,740
25R-2, 25	274.17	117,690	18,346	11,251	4,901	2,353	6,256
25R-5, 22	276.99	133,745	19,664	11,756	3,734	2,703	7,262
25R-6, 57	278.70	109,095	15,448	8,593	3,587	2,114	5,469
26R-2, 100	284.61	67,101	20,326	25,273	1,234	6,180	15,555
27R-2, 0	292.04	114,965	17,705	10,119	3,226	2,487	5,837
27R-3, 8	292.45	509,786	46,539	8,019	0		
27R-3, 88	293.26	101,527	20,422	11,745	3,363	3,681	8,174
27R-4, 16	293.62	134,883	16,674	9,451	2,927	2,666	6,493
27R-5, 48	295.30	380,453	29,769	8,277	3,706	1,545	4,585
28R-2, 10	302.26	158,135	19,489	10,823	3,925	3,101	6,759
29R-1, 49	311.19	175,790	15,873	9,672	2,786	3,005	6,777
29R-2, 13	312.23	61,532	8,603	5,835	1,786	1,549	3,666
29R-3, 0	312.57	201,904	21,482	12,164	4,223	3,106	6,904
31R-1, 40	330.11	472,575	29,681	8,453	4,194	1,706	3,737
31R-2, 38	330.54	137,318	15,546	9,448	4,223	2,535	5,654
31R-3, 0	330.59	143,013	19,906	11,889	2,570	3,044	7,754
31R-4, 64	331.71	202,548	16,272	9,571	3,397	2,549	6,426
Unit IV - silty turbidite facies							
31R-5, 70	333.09	132,757	20,649	18,798	1,861	5,527	12,581
32R-1, 8	339.28	120,261	13,133	7,193	3,213	1,540	3,774
32R-2, 41	340.54	50,223	7,685	4,662	2,932	1,499	3,260
32R-3, 23	341.05	142,892	17,117	9,215	4,087	2,287	6,072
33R-2, 0	349.21	296,716	6,696	3,345	4,085		
33R-4, 26	351.28	98,307	14,669	8,758	4,072	2,470	5,460
33R-5, 12	352.39	99,393	14,172	6,965	4,120	1,737	3,652
33R-5, 80	353.07	259,757	18,082	4,278	4,882		
34R-1, 23	357.23	167,887	20,313	9,876	4,036	2,669	6,348
34R-1, 72	357.72	128,922	17,977	10,777	3,292	2,906	6,506
34R-3, 0	359.54	138,588	16,636	8,858	3,444	2,364	5,675
35R-2, 65	367.46	137,597	16,983	9,716	3,177	2,090	5,746
36R-2, 34	376.51	154,610	20,756	11,609	4,066	2,836	7,186
36R-3, 29	376.82	169,806	14,618	9,098	3,178	2,168	5,682
37R-1, 44	385.94	149,023	17,412	15,729	3,222	4,246	11,174

Table T2 (continued).

Core, section, interval (cm)	Depth CSF (m)	Integrated peak area (total counts)					
		Smectite (001)	Illite (001)	Chlorite (002) + kaolinite (001)	Quartz (100)	Half peak chlorite (004)	Kaolinite (002) + chlorite (004)
37R-2, 0	386.30	128,247	20,278	20,269	3,226	5,651	14,169
38R-1, 95	395.95	181,501	22,271	26,263	3,572	6,362	17,145
39R-1, 118	405.68	156,991	18,203	21,974	3,390	4,480	14,419
39R-2, 37	406.23	134,398	17,715	24,660	3,526	5,896	15,101
39R-2, 73	406.59	98,657	17,004	23,726	3,627	6,600	15,286
39R-3, 35	407.25	214,283	24,656	31,539	3,857	7,310	18,269
40R-1, 21	414.21	144,437	17,005	9,054	4,564	1,987	4,937
Unit V - siliciclastic/volcaniclastic turbidite facies							
40R-3, 26	416.98	45,502	4,578	3,984	1,956	1,452	3,063
40R-4, 30	417.71	137,445	13,756	6,340	2,854	1,441	3,468
40R-5, 45	418.55	204,764	18,266	9,883	3,344	2,624	5,637
41R-1, 23	423.73	178,663	14,848	5,053	1,762	915	2,802
41R-2, 0	424.88	130,852	13,344	5,421	2,601	1,092	2,761
41R-3, 0	426.07	154,714	12,002	5,485	3,308	1,506	3,535
41R-4, 38	426.89	293,703	18,570	5,508	3,463	1,521	3,469
42R-2, 29	434.24	244,518	19,600	5,374	3,988	1,284	2,750
42R-3, 18	434.84	167,010	16,342	8,674	3,225	2,682	5,621
42R-3, 76	435.42	148,784	18,294	5,095	6,336		
43R-1, 114	443.64	143,535	13,527	7,597	3,873	2,084	4,746
43R-2, 85	444.75	176,114	15,191	6,991	3,895	1,595	3,865
43R-4, 41	446.40	299,999	24,185	9,795	4,613	2,366	5,100
44R-1, 16	452.16	230,179	16,253	6,520	5,356	1,510	3,245
44R-1, 94	452.94	134,345	13,089	7,253	4,624	2,063	4,729
44R-2, 0	453.26	74,335	6,023	4,421	5,502	1,033	2,305
45R-2, 22	463.03	1,611,840	17,210	3,457	61,145		
45R-2, 74	463.55	119,016	12,815	7,580	5,688	1,272	3,208
45R-3, 46	464.55	531,869	22,074	6,446	8,912	883	2,244
45R-4, 76	465.55	749,785	15,059	4,914	15,941		
46R-2, 0	471.36	596,795	30,980	7,581	10,500		
46R-3, 109	473.02	123,286	13,577	9,478	3,157	2,271	5,325
47R-2, 30	474.45	73,364	6,590	1,940	2,987	480	1,438
47R-3, 10	481.07	109,248	7,579	2,757	2,879	447	1,123
48R-1, 10	481.22	123,017	14,033	6,763	2,895	1,727	3,856
48R-2, 0	490.10	18,408	6,803	4,421	1,111	1,314	3,236
49R-2, 37	500.30	62,062	15,713	6,835	2,482	2,029	4,961
49R-3, 22	500.54	119,816	20,638	7,955	1,935	1,849	4,164
50R-2, 40	509.69	420,922	11,231	5,156	4,125	1,188	2,762
50R-3, 50	510.21	58,677	12,888	7,164	1,689	1,973	4,168

Table T3. Calculated values of relative mineral abundance (<2 µm size fraction) for mudstone samples, Sites C0011 and C0012. (Continued on next four pages.)

		Relative mineral abundance within clay-size fraction SVD normalization factors (wt%)						Area % within clay-size fraction Biscaye (1965) weighting factors			Relative abundance within bulk sediment (wt%)		
Core, section, interval (cm)	Depth CSF (m)	Smectite	Illite	Kaolinite + chlorite	Quartz	Kaolinite	Chlorite	Smectite	Illite	Kaolinite + chlorite	Total clay minerals	Smectite	Illite
322-C0011B-													
Unit II - volcanic turbidite facies													
1R-1, 41	340.41	61	29	9	1	2	7	53	36	11	71	44	21
1R-2, 25	341.43	56	33	10	1	1	8	48	40	12	69	39	23
3R-2, 25	359.86	45	37	11	7	3	8	39	47	13	69	33	27
3R-4, 118	362.73	60	32	8	0	1	7	51	38	11	69	41	22
3R-5, 18	363.15	60	31	9	0	2	7	51	37	12	72	43	22
4R-2, 45	366.66	84	12	4	0	1	3	74	18	8	65	55	8
4R-3, 0	366.94	82	15	4	0	1	3	71	21	8	60	49	9
5R-2, 25	375.62	87	11	1	0	0	1	76	18	7	40	35	5
5R-4, 105	378.02	50	32	12	6	7	5	44	41	15	70	37	24
6R-2, 70	386.11	58	26	14	1	4	10	51	33	16	66	39	18
6R-3, 105	387.87	57	30	10	3	4	7	50	37	13	67	40	21
6R-5, 25	388.68	57	28	12	3	4	8	51	35	14	73	43	21
6R-8, 15	391.92	63	27	8	1	2	6	55	34	11	63	40	17
7R-1, 38	393.88	48	36	13	3	4	9	42	44	15	67	33	25
7R-2, 7	394.98	83	9	2	7			83	13	5	48	43	4
7R-3, 0	395.14	87	7	0	5	0	0	86	11	3	53	49	4
7R-5, 101	397.85	58	26	10	5	1	9	53	34	13	71	44	20
8R-2, 0	404.27	92	8	0	0			83	12	4	56	51	4
8R-3, 19	404.78	72	22	6	0	1	5	62	28	9	55	40	12
8R-5, 104	408.50	56	35	9	0	2	7	47	41	12	67	37	23
8R-6, 107	409.89	80	17	3	0	0	3	69	24	8	57	45	10
9R-1, 32	412.82	55	34	10	1	1	9	47	40	13	62	34	21
9R-2, 0	413.63	96	4	0	0	0	0	88	9	2	50	48	2
10R-1, 32	422.32	61	28	10	1	1	8	53	34	12	69	43	19
10R-3, 0	424.75	54	34	11	2	2	9	46	41	13	66	36	23
11R-2, 85	433.75	70	25	5	0	0	4	60	32	8	69	48	17
11R-4, 0	434.64	84	2	0	14			100	0	0	89	87	2
11R-5, 107	436.31	64	28	7	1	0	7	55	35	10	73	47	21
11R-7, 132	439.38	60	30	8	2	0	8	52	37	11	65	39	20
12R-2, 50	442.91	67	26	7	0	2	5	58	32	10	67	45	18
12R-3, 75	444.58	64	26	9	1	2	7	56	33	12	68	44	18
12R-4, 62	445.87	56	29	12	4	2	10	50	36	14	67	39	20
12R-6, 0	446.96	66	20	9	5	2	7	61	27	12	57	40	12
12R-7, 83	448.16	64	28	7	1	1	7	55	34	10	68	44	19
13R-3, 30	453.62	61	28	10	2	1	9	53	35	12	70	43	20
13R-4, 51	454.19	60	29	11	1	4	6	52	35	13	71	43	21
13R-5, 26	455.35	61	24	14	0	5	9	53	30	16	74	46	18
14R-2, 17	461.59	61	29	8	2	2	6	53	36	11	71	44	21
14R-4, 0	463.16	71	20	9	0	2	6	62	26	12	56	40	11
14R-5, 45	464.07	81	13	6	0	2	4	70	19	11	46	38	6
14R-6, 4	465.08	52	31	12	5	2	10	47	39	14	69	38	22
15R-2, 45	471.35	62	26	12	0	3	9	53	32	15	69	42	18
15R-3, 0	472.03	37	36	19	9	5	14	33	46	21	72	29	28
15R-4, 117	473.72	50	28	16	6	2	13	46	36	18	66	36	20
16R-2, 0	478.21	87	11	2	0	1	2	75	17	8	41	35	5
	Average:	65	24	8	2	2	7	58	31	11	65	42	16
	StDev:	14	9	4	3	2	3	14	11	4	9	9	7
Unit III - hemipelagic facies													
19R-3, 0	492.65	51	28	15	6	4	11	47	36	17	71	39	21
19R-4, 20	493.22	51	30	15	4	4	11	46	38	17	71	38	22
19R-4, 74	493.76	54	28	17	1	4	14	47	34	19	72	39	20
19R-5, 32	494.72	57	30	12	1	5	7	49	36	14	72	41	22
19R-6, 19	495.95	49	31	16	4	2	14	44	38	18	73	37	23
21R-2, 0	501.65	42	32	17	9	6	11	38	43	20	71	33	25
21R-4, 106	504.73	47	33	16	5	3	13	41	41	18	71	35	24
21R-5, 130	506.38	55	31	13	2	3	10	48	37	15	72	40	23
23R-2, 0	521.15	58	29	11	3	3	8	51	36	13	70	42	21
23R-3, 117	522.74	59	30	8	2	2	7	52	37	11	67	41	21
23R-4, 30	523.27	59	28	11	2	3	8	51	35	14	72	43	21
23R-7, 106	527.36	65	28	6	0	1	5	56	34	10	72	47	20
23R-8, 53	528.24	56	27	14	3	3	11	50	34	16	72	41	20
24R-1, 0	529.90	58	28	12	3	4	8	51	35	14	71	42	20
24R-2, 17	530.64	44	32	17	7	4	13	40	41	19	70	33	24

Table T3 (continued). (Continued on next page.)

Core, section, interval (cm)	Depth CSF (m)	Relative mineral abundance within clay-size fraction SVD normalization factors (wt%)						Area % within clay-size fraction Biscaye (1965) weighting factors			Relative abundance within bulk sediment (wt%)		
		Smectite	Illite	Kaolinite + chlorite	Quartz	Kaolinite	Chlorite	Smectite	Illite	Kaolinite + chlorite	Total clay minerals	Smectite	Illite
25R-1, 30	539.70	46	29	19	6	3	16	42	37	21	71	35	22
25R-2, 50	540.36	84	12	4	0	1	3	74	18	8	61	51	7
25R-3, 22	540.71	51	32	14	2	4	10	44	39	16	69	36	23
26R-1, 112	550.12	56	28	13	4	3	9	50	35	15	71	41	20
26R-2, 67	550.89	55	29	12	5	3	8	49	37	14	64	37	19
26R-3, 25	551.27	61	28	10	2	1	9	53	34	13	72	44	20
26R-5, 104	554.72	58	27	10	5	2	9	52	35	13	70	42	20
27R-1, 22	558.72	58	31	10	1	1	10	50	37	13	70	41	22
27R-2, 48	559.84	58	28	10	5	2	8	52	36	12	69	42	20
27R-3, 115	561.07	53	31	11	5	1	10	48	39	13	68	38	22
27R-5, 110	563.81	53	29	11	7	2	9	48	39	13	68	39	22
28R-1, 15	568.17	55	31	10	5	1	9	49	39	13	69	40	22
28R-2, 0	569.46	69	26	5	0	0	4	59	32	9	69	48	18
30R-1, 30	580.70	61	27	9	3	3	7	54	34	12	73	46	20
30R-2, 0	581.78	58	29	11	3	3	8	51	36	13	70	42	21
31R-1, 108	587.58	60	25	9	6	3	7	55	33	12	68	43	18
31R-2, 50	588.36	89	10	1	0	1	0	78	16	6	82	73	8
31R-3, 77	589.17	76	24	0	0	0	0	65	30	5	75	57	18
32R-5, 0	601.39	60	29	8	3	3	5	53	36	11	69	43	20
33R-1, 22	605.72	54	31	10	5	2	8	48	39	12	69	40	23
33R-2, 0	605.94	57	31	8	4	1	7	51	39	11	68	40	22
35R-3, 23	627.39	65	25	8	3	1	7	58	32	10	60	40	15
35R-4, 0	628.14	50	34	8	8	1	7	45	45	10	70	38	26
35R-5, 87	629.47	60	26	10	5	3	6	55	33	12	69	44	19
35R-6, 60	630.54	66	24	7	3	1	6	59	31	10	68	46	17
35R-6, 115	631.06	54	30	10	7	2	8	49	39	12	67	39	21
35R-7, 94	632.21	64	25	8	3	1	7	57	32	11	74	49	19
35R-8, 44	633.08	71	23	5	0	1	4	62	29	9	69	49	16
36R-2, 50	635.17	66	25	6	3	0	6	59	32	9	69	47	18
36R-4, 127	637.89	50	29	11	9	3	8	47	40	13	71	39	23
36R-5, 69	638.72	59	31	10	0	2	8	50	37	13	71	42	22
37R-2, 50	645.18	62	25	8	5	2	6	56	33	11	74	48	20
37R-4, 9	646.61	66	23	8	3	1	7	59	30	11	69	47	16
37R-7, 33	650.81	66	25	8	1	0	7	58	32	11	70	47	18
38R-1, 72	653.72	36	32	15	17	8	7	33	49	18	71	31	27
38R-2, 0	654.39	60	26	8	6	1	7	55	34	11	68	43	19
38R-4, 64	656.98	65	24	8	3	2	6	58	31	11	56	37	14
38R-7, 92	661.49	70	23	6	0	0	6	61	30	9	65	46	15
39R-1, 23	662.74	65	24	8	3	1	7	58	31	11	64	43	16
39R-4, 50	667.24	48	27	12	13	5	7	46	39	15	68	38	21
39R-5, 108	668.41	69	23	6	2	0	6	61	29	9	62	44	14
39R-6, 25	669.00	65	24	6	5	1	5	60	32	8	71	49	18
40R-2, 17	673.57	71	23	5	1	1	4	62	29	8	69	49	16
	Average:	59	27	10	4	2	8	52	35	13	69	42	20
	StDev:	9	4	4	3	2	3	8	5	3	4	6	4
Unit IV - silty turbidite facies													
40R-3, 0	674.82	57	26	9	8	1	8	53	35	11	69	42	20
42R-2, 0	681.88	65	22	5	8	0	5	62	30	8	68	48	16
43R-2, 40	685.81	67	22	10	1	3	8	59	28	13	66	45	15
43R-3, 0	685.87	73	20	4	3	1	3	66	27	7	66	50	14
43R-4, 56	686.36	64	21	6	9	0	5	62	30	8	59	41	14
43R-5, 117	687.27	57	26	10	7	3	8	52	34	13	72	44	20
44R-2, 0	690.41	62	19	5	14	2	2	65	29	6	64	46	14
44R-3, 0	691.09	69	22	5	4	1	4	63	29	8	70	50	16
44R-4, 21	691.90	69	21	5	5	0	4	64	29	7	69	50	15
45R-1, 24	698.74	73	21	5	1	1	5	64	27	9	69	51	14
45R-3, 0	700.28	49	26	11	14	2	10	48	38	14	69	39	21
45R-4, 36	701.18	67	23	7	3	3	5	60	29	10	64	44	15
45R-8, 12	706.66	59	27	14	1	5	9	51	33	16	66	39	18
46R-1, 105	709.05	77	14	8	1	5	4	69	19	12	65	50	9
46R-2, 25	709.65	56	24	16	4	7	9	51	31	19	42	25	11
47R-3, 33	713.52	53	25	16	7	5	10	49	32	18	76	44	20
47R-3, 36	713.56	54	26	16	4	4	12	48	33	18	73	41	20
47R-4, 60	715.20	71	19	9	1	1	8	63	25	12	76	55	15
47R-5, 83	716.85	49	30	20	1	7	14	43	36	22	73	36	22
47R-5, 113	717.15	51	27	19	3	5	14	45	34	21	75	39	21

Table T3 (continued). (Continued on next page.)

Core, section, interval (cm)	Depth CSF (m)	Relative mineral abundance within clay-size fraction SVD normalization factors (wt%)						Area % within clay-size fraction Biscaye (1965) weighting factors			Relative abundance within bulk sediment (wt%)		
		Smectite	Illite	Kaolinite + chlorite	Quartz	Kaolinite	Chlorite	Smectite	Illite	Kaolinite + chlorite	Total clay minerals	Smectite	Illite
48R-3, 25	722.79	62	24	13	1	3	10	54	30	16	76	48	19
50R-2, 29	739.11	69	21	11	0	4	6	60	27	14	73	50	15
51R-1, 136	748.76	50	26	7	17	1	6	51	41	8	71	43	23
51R-2, 58	749.31	67	23	6	5	1	5	61	30	9	73	51	17
51R-4, 0	750.51	74	20	4	2	1	4	66	26	8	71	54	14
52R-1, 60	757.56	74	21	3	2	1	2	66	27	7	76	57	16
52R-1, 113	758.04	75	20	3	2	0	3	67	26	7	75	57	15
52R-2, 11	758.40	100	0	0	0			96	4	0	85	85	0
52R-3, 95	760.49	71	22	6	1	1	5	62	28	9	74	53	16
52R-5, 82	763.00	69	22	5	3	1	4	62	29	9	72	51	17
52R-6, 0	763.34	75	19	2	3	1	1	69	25	6	73	57	14
53R-1, 82	767.05	64	20	8	8	1	7	61	28	10	74	52	16
53R-1, 112	767.24	68	21	8	3	1	7	62	27	11	70	49	15
53R-2, 0	767.30	73	19	5	3	1	4	66	26	8	71	53	14
54R-5, 44	774.68	70	20	6	4	3	4	65	26	9	68	49	14
54R-5, 70	774.94	78	15	4	3	2	2	72	20	8	51	41	8
54R-5, 110	775.34	85	12	4	0	2	2	75	17	8	44	37	5
55R-1, 27	779.27	92	2	0	6			95	4	1	49	48	1
55R-2, 0	779.50	84	9	1	6			83	14	3	34	31	3
55R-3, 77	780.87	94	6	0	0	0	0	86	11	3	30	29	2
55R-5, 23	781.85	51	16	8	25	3	4	65	27	8	39	26	8
56R-2, 0	844.53	75	21	4	0	0	4	65	27	8	72	54	15
56R-3, 100	846.03	69	22	6	4	1	5	62	29	9	70	50	16
57R-2, 96	848.77	64	19	4	13	1	3	67	28	5	70	52	15
	Average:	68	20	7	5	2	6	63	27	10	66	47	14
	StDev:	12	6	5	5	2	3	11	8	5	12	10	5
Unit V - volcaniclastic facies													
57R-4, 0	850.45	100	0	0	0			96	4	0	73	73	0
57R-5, 120	852.25	67	19	3	11	1	2	69	27	4	62	47	13
57R-6, 23	852.69	100	0	0	0			100	0	0	85	85	0
57R-6, 74	853.20	100	0	0	0	0	0	92	2	6	80	80	0
58R-1, 21	856.11	95	2	1	2	0	1	89	6	5			
58R-1, 48	856.38	100	0	0	0			96	3	1			
58R-2, 119	858.42	49	27	7	17	1	6	50	42	8			
58R-3, 0	858.47	51	30	6	12	2	4	49	44	7	67	39	23
58R-4, 40	859.27	54	27	6	12	2	4	53	40	8	66	40	20
58R-4, 100	859.84	68	20	6	6	1	5	64	27	9	66	48	14
58R-5, 0	860.23	97	0	3	0	0	3	87	2	11	75	72	0
58R-5, 72	860.91	51	30	7	12	2	5	49	42	9	60	35	20
58R-6, 44	861.87	45	34	8	13	1	7	42	49	9	60	31	23
59R-3, 0	867.48	88	1	0	12			100	0	0	92	91	1
59R-4, 45	868.44	76	9	16	0	4	11	68	13	19	51	39	4
	Average:	76	13	4	6	1	4	74	20	6	70	57	10
	StDev:	22	14	4	6	1	3	22	19	5	12	22	10
322-C0012A-													
Unit I - hemipelagic/pyroclastic facies													
1R-1, 62	0.62	81	18	1	0	0	1	70	24	6	70	56	13
2R-4, 28	64.13	40	37	20	2	7	14	35	44	21	66	27	25
3R-1, 72	70.22	53	31	16	0	5	11	46	37	18	61	32	19
4R-2, 25	80.26	47	35	18	1	5	13	40	41	19			
5R-2, 25	89.68	45	34	19	2	6	14	39	41	21	63	29	22
5R-3, 42	90.31	46	34	18	1	6	12	40	41	19	62	29	22
5R-5, 18	92.49	44	35	20	1	7	14	38	41	21	61	27	21
6R-3, 10	100.45	46	34	18	1	6	12	40	41	19	65	31	23
6R-4, 71	101.39	47	33	20	1	8	12	40	39	21	67	31	22
7R-5, 108	107.84	53	31	15	1	7	8	46	37	17	68	36	22
8R-3, 30	114.62	47	31	19	3	5	14	42	38	21	64	31	20
8R-3, 108	115.40	51	31	18	0	4	14	44	37	19	67	35	21
8R-5, 0	116.62	35	33	23	9	5	18	31	44	26	65	25	24
8R-6, 47	117.33	51	32	17	0	5	11	44	37	18	63	32	20
9R-4, 0	124.03	55	34	12	0	3	9	46	39	14	72	40	24
9R-5, 59	124.86	51	33	15	0	4	11	44	39	17	70	36	23
9R-6, 30	125.98	55	31	14	0	5	9	47	37	16	62	34	19
10R-2, 41	132.03	62	25	7	6	1	6	57	34	9	70	46	19
10R-3, 44.5	132.62	56	32	12	0	3	9	48	38	14	75	42	24
10R-5, 35	134.39	50	38	11	0	3	8	42	44	14	74	37	28

Table T3 (continued). (Continued on next page.)

Core, section, interval (cm)	Depth CSF (m)	Relative mineral abundance within clay-size fraction SVD normalization factors (wt%)						Area % within clay-size fraction Biscaye (1965) weighting factors			Relative abundance within bulk sediment (wt%)		
		Smectite	Illite	Kaolinite + chlorite	Quartz	Kaolinite	Chlorite	Smectite	Illite	Kaolinite + chlorite	Total clay minerals	Smectite	Illite
10R-5, 92	134.96	65	27	7	0	2	6	56	33	11	64	42	17
10R-6, 0	135.44	46	35	14	5	3	11	40	44	16	64	31	24
11R-3, 24	142.89	56	30	13	1	2	11	49	36	15	63	36	19
11R-4, 0	144.03	64	29	8	0	2	5	54	35	11	73	46	21
11R-5, 107	145.37	55	34	11	0	2	9	46	40	14	75	41	26
11R-6, 113	146.64	69	24	7	1	2	5	60	30	10	73	51	18
	Average:	53	32	14	1	4	10	46	38	16	67	36	21
	StDev:	10	4	5	2	2	4	8	5	5	5	8	3
Unit II - volcanic turbidite facies													
13R-2, 25	159.89	58	33	9	0	1	8	49	39	11	69	40	23
13R-3, 68	160.81	91	9	1	0	0	1	80	14	6	43	39	4
14R-2, 0	169.69	55	33	10	3	1	9	47	40	12	66	37	22
14R-3, 85	170.83	64	28	8	0	1	7	55	34	11	70	45	19
15R-3, 0	180.09	59	27	9	5	1	8	53	35	12	43	26	12
16R-3, 0	189.03	55	30	12	2	3	9	48	37	14	72	41	22
16R-4, 68	189.99	52	35	14	0	4	10	44	41	16	64	33	22
16R-5, 12	190.85	70	25	5	0	2	3	60	32	9	71	49	18
17R-1, 28	197.28	65	26	8	2	2	6	57	32	11	68	45	18
17R-2, 45	198.65	58	30	9	3	1	8	51	38	11	66	40	21
17R-3, 27	199.09	60	30	9	1	2	7	52	37	11	72	43	22
17R-4, 17	199.28	73	23	4	0	2	3	63	29	8	69	51	16
18R-2, 48	208.38	42	27	16	15	9	7	40	40	20	78	38	25
19R-1, 79	216.49	65	25	10	0	2	7	56	31	13	72	47	18
19R-2, 51	217.56	67	22	10	0	3	7	58	28	13	78	52	18
19R-3, 12	217.70	66	20	12	3	3	8	60	26	15	72	49	15
19R-4, 17	219.15	78	16	6	0	1	4	69	22	10	80	62	13
	Average:	63	26	9	2	2	7	55	33	12	68	43	18
	StDev:	11	7	4	4	2	2	10	7	3	10	8	5
Unit III - hemipelagic facies													
19R-4, 122	220.20	64	26	10	0	4	6	55	32	13	74	47	19
20R-3, 0	227.50	49	32	13	6	4	9	44	41	15	77	40	26
20R-4, 16	228.00	45	24	17	14	7	10	44	35	21	80	42	22
20R-4, 100	228.84	60	27	11	2	2	8	53	34	13	78	48	22
20R-5, 20	229.44	52	29	13	6	3	10	47	37	15	77	43	24
21R-1, 23	234.93	74	21	5	0	2	4	64	27	9	73	54	15
21R-2, 30	235.69	77	19	4	0	1	3	67	25	8	80	62	15
21R-3, 105	236.77	58	30	10	3	1	8	51	37	12	77	45	23
22R-1, 109	245.29	65	27	7	0	1	6	56	34	10	73	48	20
23R-2, 45	255.52	48	31	13	9	3	10	44	41	15	73	38	24
23R-3, 45	256.55	67	25	7	1	2	6	58	31	10	71	48	18
23R-5, 91	258.75	67	26	7	0	1	6	58	32	10	75	51	19
23R-6, 43	259.51	60	29	9	2	2	7	52	36	12	75	46	22
24R-1, 48	263.68	60	28	8	3	3	6	53	36	11	71	44	21
24R-2, 0	263.93	63	25	8	3	3	5	56	33	11	75	49	20
24R-3, 48	264.76	57	28	10	5	2	8	51	36	13	74	44	22
24R-4, 98	266.67	62	30	8	0	1	7	53	36	11	74	46	22
25R-1, 110	273.80	67	24	7	3	2	5	59	31	9	71	49	18
25R-2, 25	274.17	57	24	8	11	3	5	55	34	11	70	44	19
25R-5, 22	276.99	62	25	7	5	3	5	57	33	10	76	50	20
25R-6, 57	278.70	62	24	7	8	2	5	58	33	9	75	50	19
26R-2, 100	284.61	38	35	25	2	7	18	34	41	25	77	30	27
27R-2, 0	292.04	61	26	7	5	1	6	56	34	10	74	48	21
27R-3, 8	292.45	82	18	0	0			72	26	2	74	61	14
27R-3, 88	293.26	54	30	9	7	1	8	49	40	11	76	44	24
27R-4, 16	293.62	69	23	5	2	1	4	61	30	9	70	49	17
27R-5, 48	295.30	84	16	0	0	0	0	74	23	3	73	61	12
28R-2, 10	302.26	68	23	5	4	1	5	61	30	8	75	52	18
29R-1, 49	311.19	78	19	3	0	1	3	68	25	7	71	56	13
29R-2, 13	312.23	62	24	8	6	2	6	57	32	11	69	46	18
29R-3, 0	312.57	73	21	4	2	1	4	65	28	8	70	52	15
31R-1, 40	330.11	87	13	0	0	0	0	78	20	3	71	62	9
31R-2, 38	330.54	66	21	6	7	1	5	63	28	9	72	52	16
31R-3, 0	330.59	67	26	7	0	2	5	58	32	10	74	50	19
31R-4, 64	331.71	81	17	3	0	1	2	71	23	7	69	55	12
	Average:	64	25	8	3	2	6	57	32	11	74	49	19
	StDev:	11	5	5	4	2	3	9	5	4	3	7	4

Table T3 (continued).

		Relative mineral abundance within clay-size fraction SVD normalization factors (wt%)						Area % within clay-size fraction Biscaye (1965) weighting factors			Relative abundance within bulk sediment (wt%)		
Core, section, interval (cm)	Depth CSF (m)	Smectite	Illite	Kaolinite + chlorite	Quartz	Kaolinite	Chlorite	Smectite	Illite	Kaolinite + chlorite	Total clay minerals	Smectite	Illite
Unit IV - silty turbidite facies													
31R-5, 70	333.09	61	27	12	0	2	10	52	33	15	70	43	19
32R-1, 8	339.28	69	21	5	5	1	4	64	28	8	77	56	17
32R-2, 41	340.54	54	22	8	16	1	7	56	34	10	63	40	17
32R-3, 23	341.05	67	22	5	6	2	4	62	30	8	73	52	17
33R-2, 0	349.21	97	3	0	0			90	8	2	90	87	3
33R-4, 26	351.28	58	24	8	11	1	7	56	34	10	64	41	17
33R-5, 12	352.39	59	23	6	11	0	6	58	33	8	70	47	18
33R-5, 80	353.07	85	15	0	0			76	21	3	69	59	11
34R-1, 23	357.23	69	23	4	3	1	3	62	30	7	70	50	17
34R-1, 72	357.72	64	25	7	4	1	6	58	32	10	71	47	18
34R-3, 0	359.54	68	23	5	4	1	4	62	30	8	66	47	16
35R-2, 65	367.46	68	23	6	3	2	4	61	30	9	70	49	17
36R-2, 34	376.51	65	24	6	5	2	4	59	32	9	73	50	18
36R-3, 29	376.82	78	18	4	0	1	3	69	24	7	78	61	14
37R-1, 44	385.94	67	21	10	2	3	6	60	28	13	69	47	15
37R-2, 0	386.30	57	25	14	4	4	10	51	32	16	66	39	17
38R-1, 95	395.95	63	22	14	2	5	9	56	28	16	71	46	16
39R-1, 118	405.68	64	21	13	3	7	7	57	27	16	72	47	15
39R-2, 37	406.23	57	21	17	5	5	12	53	28	19	67	40	15
39R-2, 73	406.59	49	24	19	9	4	15	46	32	22	76	41	20
39R-3, 35	407.25	65	21	14	1	4	10	57	26	17	73	47	15
40R-1, 21	414.21	66	21	5	7	1	4	63	30	8	78	55	18
	Average:	66	21	8	5	2	7	60	29	11	72	50	16
	StDev:	10	5	5	4	2	3	9	6	5	6	10	3
Unit V - siliciclastic/volcaniclastic turbidite facies													
40R-3, 26	416.98	62	18	8	12	1	8	63	26	11	80	56	16
40R-4, 30	417.71	75	20	3	1	1	2	67	27	6	79	61	16
40R-5, 45	418.55	79	19	3	0	0	2	69	25	7	76	60	14
41R-1, 23	423.73	83	17	0	0	0	0	72	24	4	70	58	12
41R-2, 0	424.88	76	21	2	1	1	1	67	27	6	82	63	17
41R-3, 0	426.07	80	16	2	2	0	1	72	22	5	79	64	13
41R-4, 38	426.89	87	13	0	0	0	0	77	20	3	80	69	10
42R-2, 29	434.24	83	17	0	0	0	0	73	23	3	71	59	12
42R-3, 18	434.84	76	20	3	1	0	3	67	26	7	73	56	15
42R-3, 76	435.42	63	22	3	12			64	32	4	48	34	12
43R-1, 114	443.64	72	19	4	5	1	4	67	25	7	33	25	6
43R-2, 85	444.75	78	18	2	2	1	2	70	24	6	66	52	12
43R-4, 41	446.40	83	17	0	0	0	0	72	23	5	75	62	13
44R-1, 16	452.16	81	15	1	3	0	1	75	21	4	48	40	7
44R-1, 94	452.94	68	18	5	9	1	4	67	26	7	72	54	15
44R-2, 0	453.26	57	14	7	21	1	6	69	22	8	71	51	13
45R-2, 22	463.03	84	4	0	12			96	4	0	42	41	2
45R-2, 74	463.55	61	19	6	14	2	5	64	28	8	62	44	13
45R-3, 46	464.55	92	8	0	0	0	0	84	14	2	52	47	4
45R-4, 76	465.55	95	4	0	1			91	7	1	41	39	1
46R-2, 0	471.36	89	11	0	0			81	17	2	59	53	7
46R-3, 109	473.02	68	21	7	4	1	5	63	28	10	70	50	15
47R-2, 30	474.45	68	17	2	12	1	1	71	25	4	29	23	6
47R-3, 10	481.07	79	15	1	5	0	1	75	21	4	74	62	12
48R-1, 10	481.22	71	22	4	3	1	3	64	29	7	71	52	16
48R-2, 0	490.10	38	36	14	13	4	10	34	50	16	55	24	22
49R-2, 37	500.30	49	34	8	9	2	6	45	45	10	78	42	29
49R-3, 22	500.54	65	31	4	0	1	3	55	38	7	76	49	24
50R-2, 40	509.69	97	3	0	0	0	0	88	9	2	85	82	3
50R-3, 50	510.21	53	32	9	5	1	8	47	41	12	69	39	24
	Average:	74	18	3	5	1	3	69	25	6	66	50	13
	StDev:	14	8	3	6	1	3	13	10	4	15	14	7

SVD = singular value decomposition. StDev = standard deviation.

Table T4. Results of X-ray diffraction analysis (<2 µm size fraction) with values of illite/smectite (I/S) expandability, illite in I/S, and illite crystallinity index, Sites C0011 and C0012. (Continued on next four pages.)

Core, section interval (cm)	Depth CSF (m)	Intensity saddle (cps)	Intensity peak (cps)	Ratio saddle peak	Expandability (%)	Illite (002)/ smectite (003) d (Å)	Illite in I/S (%)	Illite crystallinity (Δ°2θ)
322-C0011B-								
Unit II - volcanic turbidite facies								
1R-1, 41	340.41	456	1295	0.352	79	15.83	14	0.35
1R-2, 25	341.43	719	1593	0.451	73	15.80	10	0.34
3R-2, 25	359.86	338	666	0.508	71	15.77	9	0.37
3R-4, 118	362.73	656	1397	0.470	72	15.78	9	0.36
3R-5, 18	363.15	559	1358	0.412	76	15.67	6	0.34
4R-2, 45	366.66	452	1548	0.292	79	15.75	8	0.38
4R-3, 0	366.94	608	1812	0.336	76	15.61	3	0.33
5R-2, 25	375.62	505	2096	0.241	82	15.66	5	0.40
5R-4, 105	378.02	274	572	0.479	72	15.93	23	0.62
6R-2, 70	386.11	568	1350	0.421	75	15.79	10	0.35
6R-3, 105	387.87	688	1544	0.446	74	15.54	1	0.35
6R-5, 25	388.68	620	1458	0.425	75	15.99	27	0.41
6R-8, 15	391.92	449	1146	0.392	77	15.87	19	0.35
7R-1, 38	393.88	221	514	0.430	75	15.67	6	0.41
7R-2, 7	394.98	180	645	0.279	80	15.66	5	0.50
7R-3, 0	395.14	213	939	0.227	83	15.60	3	0.61
7R-5, 101	397.85	428	1019	0.420	75	15.94	24	0.41
8R-2, 0	404.27	252	955	0.264	81	15.65	5	0.61
8R-3, 19	404.78	375	1160	0.323	77	15.68	6	0.37
8R-5, 104	408.50	779	1553	0.502	71	15.82	13	0.36
8R-6, 107	409.89	523	1668	0.314	78	15.67	6	0.39
9R-1, 32	412.82	565	1129	0.500	71	15.87	19	0.34
9R-2, 0	413.63	362	2451	0.148	90	15.76	9	0.54
10R-1, 32	422.32	707	1654	0.427	75	15.64	4	0.31
10R-3, 0	424.75	846	1623	0.521	70	15.73	8	0.35
11R-2, 85	433.75	712	2013	0.354	79	15.78	9	0.38
11R-4, 0	434.64	175	419	0.418	72	15.65	5	
11R-5, 107	436.31	619	1553	0.399	76	15.67	6	0.35
11R-7, 132	439.38	546	1412	0.387	77	15.79	10	0.39
12R-2, 50	442.91	615	1584	0.388	77	15.80	10	0.39
12R-3, 75	444.58	501	1254	0.400	76	15.81	11	0.33
12R-4, 62	445.87	552	1278	0.432	74	15.89	21	0.34
12R-6, 0	446.96	241	956	0.252	82	15.78	9	0.43
12R-7, 83	448.16	547	1476	0.371	78	15.69	6	0.42
13R-3, 30	453.62	643	1754	0.367	78	15.82	13	0.42
13R-4, 51	454.19	752	1692	0.444	74	15.79	10	0.34
13R-5, 26	455.35	600	1411	0.425	75	15.83	14	0.33
14R-2, 17	461.59	549	1528	0.359	79	15.79	10	0.41
14R-4, 0	463.16	641	1958	0.327	77	15.72	7	0.35
14R-5, 45	464.07	684	2806	0.244	82	15.68	6	0.37
14R-6, 4	465.08	352	929	0.379	78	15.70	7	0.34
15R-2, 45	471.35	634	1461	0.434	74	15.68	6	0.36
15R-3, 0	472.03	205	572	0.358	79	15.82	13	0.66
15R-4, 117	473.72	482	1120	0.430	75	15.85	16	0.34
16R-2, 0	478.21	420	2085	0.201	85	15.65	5	0.35
				Average:	77		10	
Unit III - hemipelagic facies								
19R-3, 0	492.65	441	1040	0.424	75	15.77	9	0.39
19R-4, 20	493.22	678	1334	0.508	71	15.78	9	0.35
19R-4, 74	493.76	715	1579	0.453	73	15.82	13	0.36
19R-5, 32	494.72	727	1878	0.387	77	15.66	5	0.35
19R-6, 19	495.95	647	1322	0.489	71	15.85	16	0.31
21R-2, 0	501.65	340	780	0.436	74	15.90	21	0.43
21R-4, 106	504.73	465	1064	0.437	74	15.88	20	0.41
21R-5, 130	506.38	702	1618	0.434	74	15.88	20	0.38
23R-2, 0	521.15	621	1522	0.408	76	15.81	11	0.35
23R-3, 117	522.74	457	1110	0.412	76	15.76	9	0.32
23R-4, 30	523.27	667	1566	0.426	75	15.73	8	0.34
23R-7, 106	527.36	705	2393	0.295	83	15.69	6	0.52
23R-8, 53	528.24	608	1315	0.462	73	15.88	20	0.30
24R-1, 0	529.90	584	1586	0.368	78	15.80	10	0.34
24R-2, 17	530.64	390	936	0.417	75	15.81	11	0.37
25R-1, 30	539.70	459	1049	0.438	74	15.79	10	0.40
25R-2, 50	540.36	512	2480	0.206	85	15.59	3	0.38

Table T4 (continued). (Continued on next page.)

Core, section interval (cm)	Depth CSF (m)	Intensity saddle (cps)	Intensity peak (cps)	Ratio saddle peak	Expandability (%)	Illite (002)/ smectite (003) d (Å)	Illite in I/S (%)	Illite crystallinity (Δ°2θ)
25R-3, 22	540.71	619	1386	0.447	74	15.81	11	0.36
26R-1, 112	550.12	491	1228	0.400	76	15.95	25	0.43
26R-2, 67	550.89	535	1279	0.418	75	15.81	11	0.33
26R-3, 25	551.27	654	1523	0.429	75	15.89	21	0.35
26R-5, 104	554.72	510	1194	0.427	75	15.83	14	0.33
27R-1, 22	558.72	683	1703	0.401	76	15.78	9	0.33
27R-2, 48	559.84	485	1174	0.413	76	15.72	7	0.34
27R-3, 115	561.07	617	1325	0.466	73	15.90	21	0.33
27R-5, 110	563.81	383	912	0.420	75	15.84	15	0.42
28R-1, 15	568.17	435	1169	0.372	78	15.88	20	0.41
28R-2, 0	569.46	814	2564	0.317	81	15.82	13	0.44
30R-1, 30	580.70	774	1624	0.477	72	15.81	11	0.34
30R-2, 0	581.78	534	1380	0.387	77	15.81	11	0.46
31R-1, 108	587.58	544	1371	0.397	76	15.80	10	0.37
31R-2, 50	588.36	528	2164	0.244	82	15.67	6	0.34
31R-3, 77	589.17	420	1987	0.211	85	15.84	15	0.75
32R-5, 0	601.39	540	1224	0.441	74	15.70	7	0.47
33R-1, 22	605.72	306	873	0.351	79	15.89	21	0.54
33R-2, 0	605.94	649	1487	0.436	74	15.86	18	0.37
35R-3, 23	627.39	443	1307	0.339	80	15.82	13	0.40
35R-4, 0	628.14	171	864	0.198	89	15.66	5	0.70
35R-5, 87	629.47	369	1063	0.347	79	15.76	9	0.36
35R-6, 60	630.54	430	1046	0.411	76	15.89	21	0.41
35R-6, 115	631.06	574	1620	0.354	79	15.87	19	0.34
35R-7, 94	632.21	487	1433	0.340	80	15.92	23	0.47
35R-8, 44	633.08	676	1718	0.393	73	15.72	7	0.48
36R-2, 50	635.17	655	1524	0.430	75	15.73	8	0.35
36R-4, 127	637.89	397	963	0.412	76	15.69	6	0.43
36R-5, 69	638.72	641	1472	0.435	74	15.77	9	0.32
37R-2, 50	645.18	564	1323	0.426	75	15.85	16	0.33
37R-4, 9	646.61	584	1428	0.409	76	15.77	9	0.33
37R-7, 33	650.81	632	1701	0.372	78	15.91	22	0.40
38R-1, 72	653.72	230	480	0.479	72	15.84	15	0.62
38R-2, 0	654.39	586	1407	0.416	75	15.88	20	0.36
38R-4, 64	656.98	470	1264	0.372	78	15.85	16	0.41
38R-7, 92	661.49	627	1780	0.352	75	15.81	11	0.48
39R-1, 23	662.74	572	1447	0.395	77	15.80	10	0.35
39R-4, 50	667.24	248	634	0.391	77	15.75	8	0.55
39R-5, 108	668.41	687	1676	0.410	72	15.91	22	0.35
39R-6, 25	669.00	445	1405	0.317	81	15.68	6	0.39
40R-2, 17	673.57	534	1816	0.294	79	15.69	6	0.43
				Average:	77		13	
Unit IV - silty turbidite facies								
40R-3, 0	674.82	371	1012	0.367	78	15.79	10	0.43
42R-2, 0	681.88	507	1361	0.373	78	15.86	18	0.36
43R-2, 40	685.81	653	1749	0.373	74	15.74	8	0.38
43R-3, 0	685.87	695	1884	0.369	74	15.81	11	0.39
43R-4, 56	686.36	470	1242	0.378	74	15.87	19	0.38
43R-5, 117	687.27	387	931	0.416	75	15.90	21	0.41
44R-2, 0	690.41	413	1308	0.316	77	15.76	9	0.39
44R-3, 0	691.09	632	1819	0.347	75	15.87	19	0.41
44R-4, 21	691.90	528	1682	0.314	78	15.77	9	0.39
45R-1, 24	698.74	568	1777	0.320	77	15.73	8	0.43
45R-3, 0	700.28	170	569	0.299	82	15.93	23	0.74
45R-4, 36	701.18	460	1490	0.309	82	15.76	9	0.42
45R-8, 12	706.66	751	1777	0.423	75	15.83	14	0.38
46R-1, 105	709.05	434	1796	0.242	82	15.66	5	0.39
46R-2, 25	709.65	518	1413	0.367	78	15.83	14	0.44
47R-3, 33	713.52	528	1386	0.381	77	15.85	16	0.40
47R-3, 36	713.56	554	1336	0.415	75	15.82	13	0.45
47R-4, 60	715.20	560	1788	0.313	78	15.71	7	0.43
47R-5, 83	716.85	479	1191	0.402	76	15.82	13	0.45
47R-5, 113	717.15	507	1117	0.454	73	15.81	11	0.40
48R-3, 25	722.79	970	2099	0.462	73	15.78	9	0.42
50R-2, 29	739.11	718	1925	0.373	74	15.68	6	0.37
51R-1, 136	748.76	392	693	0.566	68	15.81	11	0.40
51R-2, 58	749.31	531	1504	0.353	79	15.76	9	0.41

Table T4 (continued). (Continued on next page.)

Core, section interval (cm)	Depth CSF (m)	Intensity saddle (cps)	Intensity peak (cps)	Ratio saddle peak	Expandability (%)	Illite (002)/ smectite (003) d (Å)	Illite in I/S (%)	Illite crystallinity (Δ°2θ)
51R-4, 0	750.51	512	1780	0.288	79	15.85	16	0.40
52R-1, 60	757.56	499	1650	0.302	78	15.91	22	0.54
52R-1, 113	758.04	681	1839	0.370	74	15.74	8	0.40
52R-2, 11	758.40	477	4725	0.101	95	15.51	0	0.53
52R-3, 95	760.49	677	1672	0.405	72	15.65	5	0.38
52R-5, 82	763.00	611	1719	0.355	75	15.64	4	0.40
52R-6, 0	763.34	696	2486	0.280	80	15.74	8	0.49
53R-1, 82	767.05	311	1018	0.306	78	15.74	8	0.49
53R-1, 112	767.24	704	1863	0.378	74	15.85	16	0.36
53R-2, 0	767.30	521	1679	0.310	78	15.82	13	0.51
54R-5, 44	774.68	566	1707	0.332	76	15.62	4	0.41
54R-5, 70	774.94	557	1975	0.282	80	15.62	4	0.34
54R-5, 110	775.34	570	2468	0.231	83	15.68	6	0.46
55R-1, 27	779.27	414	3486	0.119	93	15.66	5	0.46
55R-2, 0	779.50	282	1346	0.210	85	15.64	4	0.52
55R-3, 77	780.87	617	2878	0.214	84	15.64	4	0.42
55R-5, 23	781.85	159	481	0.331	76	15.67	6	0.91
56R-2, 0	844.53	708	1948	0.363	75	15.71	7	0.50
56R-3, 100	846.03	610	1645	0.371	74	15.82	13	0.38
57R-2, 96	848.77	471	1170	0.403	72	15.76	9	0.41
				Average:	78		10	
Unit V - volcaniclastic facies								
57R-4, 0	850.45	596	4692	0.127	92	15.69	6	0.45
57R-5, 120	852.25	496	1243	0.399	73	15.91	22	0.44
57R-6, 23	852.69	546	5027	0.109	94	15.73	8	
57R-6, 74	853.20	545	3813	0.143	90	15.62	4	0.40
58R-1, 21	856.11	309	1855	0.167	88	15.70	7	0.54
58R-1, 48	856.38	265	1762	0.150	90	15.75	8	0.34
58R-2, 119	858.42	358	649	0.552	69	15.97	26	0.43
58R-3, 0	858.47	569	976	0.583	67	15.69	6	0.48
58R-4, 40	859.27	419	909	0.461	73	15.70	7	0.58
58R-4, 100	859.84	526	1533	0.343	76	15.72	7	0.44
58R-5, 0	860.23	515	3094	0.166	88	15.78	9	0.34
58R-5, 72	860.91	448	785	0.571	68	15.82	13	0.57
58R-6, 44	861.87	467	728	0.641	65	15.74	8	0.51
59R-3, 0	867.48	345	5948	0.058	100	15.72	7	
59R-4, 45	868.44	440	1505	0.292	79	15.84	15	0.44
				Average:	81		10	
322-C0012A-								
Unit I - hemipelagic/pyroclastic facies								
1R-1, 62	0.62	778	2656	0.293	79	15.77	9	0.42
2R-4, 28	64.13	526	940	0.560	68	15.89	21	0.30
3R-1, 72	70.22	398	777	0.512	70	15.77	9	0.32
4R-2, 25	80.26	451	870	0.518	70	16.04	31	0.32
5R-2, 25	89.68	578	1120	0.516	70	16.02	29	0.31
5R-3, 42	90.31	712	1279	0.557	68	15.85	16	0.31
5R-5, 18	92.49	554	1055	0.525	70	15.84	15	0.32
6R-3, 10	100.45	647	1242	0.521	70	15.87	19	0.31
6R-4, 71	101.39	522	1149	0.454	73	15.84	15	0.36
7R-5, 108	107.84	629	1242	0.506	71	16.00	28	0.32
8R-3, 30	114.62	469	805	0.583	67	15.82	13	0.33
8R-3, 108	115.40	447	1025	0.436	74	15.79	10	0.39
8R-5, 0	116.62	269	505	0.533	69	15.93	23	0.49
8R-6, 47	117.33	652	1331	0.490	71	15.88	20	0.33
9R-4, 0	124.03	913	1875	0.487	72	15.84	15	0.33
9R-5, 59	124.86	621	1282	0.484	72	15.82	13	0.28
9R-6, 30	125.98	495	1139	0.435	74	15.90	21	0.33
10R-2, 41	132.03	383	1180	0.325	81	15.75	8	0.35
10R-3, 44.5	132.62	712	1541	0.462	73	15.89	21	0.35
10R-5, 35	134.39	503	939	0.536	69	16.02	29	0.43
10R-5, 92	134.96	579	1515	0.382	77	15.74	8	0.37
10R-6, 0	135.44	420	811	0.518	70	15.84	15	0.36
11R-3, 24	142.89	491	1171	0.419	75	15.83	14	0.36
11R-4, 0	144.03	775	1753	0.442	74	15.78	9	0.34
11R-5, 107	145.37	716	1551	0.462	73	15.70	7	0.31
11R-6, 113	146.64	557	1587	0.351	79	15.98	27	0.42
				Average:	72		17	

Table T4 (continued). (Continued on next page.)

Core, section interval (cm)	Depth CSF (m)	Intensity saddle (cps)	Intensity peak (cps)	Ratio saddle peak	Expandability (%)	Illite (002)/ smectite (003) d (Å)	Illite in I/S (%)	Illite crystallinity (Δ°2θ)
Unit II - volcanic turbidite facies								
13R-2, 25	159.89	597	1497	0.399	76	15.78	9	0.42
13R-3, 68	160.81	417	1797	0.232	83	15.61	3	0.32
14R-2, 0	169.69	511	1280	0.399	76	15.98	27	0.40
14R-3, 85	170.83	508	1395	0.364	78	15.70	7	0.37
15R-3, 0	180.09	362	888	0.408	76	15.92	23	0.35
16R-3, 0	189.03	609	1453	0.419	75	15.73	8	0.39
16R-4, 68	189.99	358	954	0.375	78	15.69	6	0.49
16R-5, 12	190.85	660	1851	0.357	79	15.93	23	0.42
17R-1, 28	197.28	508	1465	0.347	79	15.76	9	0.34
17R-2, 45	198.65	417	1183	0.352	79	15.73	8	0.39
17R-3, 27	199.09	640	1619	0.395	77	15.61	3	0.35
17R-4, 17	199.28	626	1774	0.353	75	15.75	8	0.37
18R-2, 48	208.38	191	434	0.440	74	15.75	8	0.43
19R-1, 79	216.49	875	2256	0.388	77	15.76	9	0.35
19R-2, 51	217.56	800	2356	0.340	80	15.70	7	0.38
19R-3, 12	217.70	506	1506	0.336	76	15.71	7	0.36
19R-4, 17	219.15	630	2430	0.259	81	15.72	7	0.45
				Average:	78		10	
Unit III - hemipelagic facies								
19R-4, 122	220.20	838	1861	0.450	73	15.70	7	0.33
20R-3, 0	227.50	384	1056	0.364	78	15.92	23	0.48
20R-4, 16	228.00	214	452	0.473	72	15.59	3	0.40
20R-4, 100	228.84	576	1579	0.365	78	15.71	7	0.34
20R-5, 20	229.44	262	607	0.432	75	15.87	19	0.75
21R-1, 23	234.93	727	2215	0.328	77	15.80	10	0.35
21R-2, 30	235.69	670	2295	0.292	79	15.83	14	0.35
21R-3, 105	236.77	516	1349	0.383	77	15.97	26	0.34
22R-1, 109	245.29	514	1530	0.336	80	15.76	9	0.35
23R-2, 45	255.52	420	913	0.460	73	15.75	8	0.40
23R-3, 45	256.55	698	1706	0.409	76	15.78	9	0.36
23R-5, 91	258.75	579	1370	0.423	75	15.72	7	0.43
23R-6, 43	259.51	597	1541	0.387	77	15.82	13	0.40
24R-1, 48	263.68	465	1267	0.367	78	15.65	5	0.43
24R-2, 0	263.93	608	1597	0.381	77	15.87	19	0.41
24R-3, 48	264.76	418	1173	0.356	79	15.70	7	0.44
24R-4, 98	266.67	837	2185	0.383	77	15.88	20	0.39
25R-1, 110	273.80	501	1650	0.304	82	15.67	6	0.38
25R-2, 25	274.17	434	1239	0.350	79	15.68	6	0.34
25R-5, 22	276.99	413	1348	0.306	82	15.81	11	0.41
25R-6, 57	278.70	393	1143	0.344	80	15.74	8	0.39
26R-2, 100	284.61	428	753	0.568	68			0.33
27R-2, 0	292.04	374	1166	0.321	81	15.79	10	0.49
27R-3, 8	292.45	819	4091	0.200	85	15.83	14	0.98
27R-3, 88	293.26	320	954	0.335	80	15.78	9	0.46
27R-4, 16	293.62	448	1348	0.332	80	15.77	9	0.38
27R-5, 48	295.30	635	3149	0.202	85	15.86	18	0.76
28R-2, 10	302.26	596	1603	0.372	78	15.74	8	0.34
29R-1, 49	311.19	668	1803	0.370	74	15.71	7	0.35
29R-2, 13	312.23	241	643	0.375	78	15.77	9	0.47
29R-3, 0	312.57	636	1986	0.320	77	15.70	7	0.38
31R-1, 40	330.11	947	4104	0.231	83	15.73	8	0.82
31R-2, 38	330.54	454	1379	0.329	77	15.76	9	0.32
31R-3, 0	330.59	691	1510	0.458	73	15.67	6	0.33
31R-4, 64	331.71	670	2041	0.328	77	15.68	6	0.34
				Average:	78		11	
Unit IV - silty turbidite facies								
31R-5, 70	333.09	456	1357	0.336	80	15.71	7	0.32
32R-1, 8	339.28	357	1206	0.296	79	15.80	10	0.55
32R-2, 41	340.54	209	553	0.378	78	15.76	9	0.32
32R-3, 23	341.05	456	1444	0.316	77	15.80	10	0.35
33R-2, 0	349.21	416	3144	0.132	91	15.67	6	0.56
33R-4, 26	351.28	508	1165	0.436	74	15.76	9	0.28
33R-5, 12	352.39	353	1029	0.343	80	15.73	8	0.43
33R-5, 80	353.07	712	2469	0.288	79	15.76	9	0.82
34R-1, 23	357.23	519	1661	0.312	78	15.78	9	0.42

Table T4 (continued).

Core, section interval (cm)	Depth CSF (m)	Intensity saddle (cps)	Intensity peak (cps)	Ratio saddle peak	Expandability (%)	Illite (002)/ smectite (003) d (Å)	Illite in I/S (%)	Illite crystallinity (Δ°2θ)
34R-1, 72	357.72	440	1343	0.328	81	15.76	9	0.41
34R-3, 0	359.54	513	1455	0.353	75	15.68	6	0.34
35R-2, 65	367.46	470	1365	0.344	80	15.67	6	0.37
36R-2, 34	376.51	466	1514	0.308	82	15.72	7	0.46
36R-3, 29	376.82	546	1814	0.301	78	15.67	6	0.37
37R-1, 44	385.94	700	1559	0.449	70	15.74	8	0.34
37R-2, 0	386.30	439	1312	0.335	80	15.85	16	0.40
38R-1, 95	395.95	607	1760	0.345	80	15.83	14	0.48
39R-1, 118	405.68	603	1642	0.367	74	15.83	14	0.43
39R-2, 37	406.23	526	1448	0.363	78	15.71	7	0.35
39R-2, 73	406.59	435	1084	0.401	76	15.62	4	0.33
39R-3, 35	407.25	701	2148	0.326	77	15.64	4	0.46
40R-1, 21	414.21	424	1433	0.296	79	15.78	9	0.41
				Average:	78		9	
Unit V - siliciclastic/volcaniclastic turbidite facies								
40R-3, 26	416.98	223	551	0.405	72	15.66	5	0.52
40R-4, 30	417.71	445	1321	0.337	76	15.78	9	0.46
40R-5, 45	418.55	706	2037	0.347	76	15.81	11	0.40
41R-1, 23	423.73	463	1592	0.291	79	15.67	6	0.67
41R-2, 0	424.88	368	1227	0.300	78	15.83	14	0.50
41R-3, 0	426.07	576	1623	0.355	75	15.78	9	0.33
41R-4, 38	426.89	661	2621	0.252	82	15.72	7	0.66
42R-2, 29	434.24	767	2376	0.323	77	15.81	11	0.39
42R-3, 18	434.84	562	1720	0.327	77	15.71	7	0.38
42R-3, 76	435.42	341	1379	0.247	86	15.82	13	0.77
43R-1, 114	443.64	462	1478	0.313	78	15.82	13	0.36
43R-2, 85	444.75	540	1734	0.311	78	15.67	6	0.41
43R-4, 41	446.40	666	2714	0.245	82	15.78	9	0.46
44R-1, 16	452.16	643	2359	0.273	80	15.76	9	0.42
44R-1, 94	452.94	534	1472	0.363	75	15.76	9	0.32
44R-2, 0	453.26	274	883	0.310	78	15.59	3	0.24
45R-2, 22	463.03	677	21307	0.032	103	15.67	6	0.65
45R-2, 74	463.55	402	1319	0.305	78	15.76	9	0.25
45R-3, 46	464.55	701	5310	0.132	91	15.73	8	0.57
45R-4, 76	465.55	677	9491	0.071	98	15.66	5	0.53
46R-2, 0	471.36	804	5637	0.143	90	15.75	8	0.84
46R-3, 109	473.02	535	1330	0.402	72	15.77	9	0.34
47R-2, 30	474.45	279	1104	0.253	82	15.82	13	0.47
47R-3, 10	481.07	334	1599	0.209	85	15.80	10	0.50
48R-1, 10	481.22	539	1264	0.426	71	15.76	9	0.38
48R-2, 0	490.10	169	284	0.595	67	16.07	35	0.65
49R-2, 37	500.30	426	733	0.581	67	15.79	10	0.43
49R-3, 22	500.54	763	1358	0.562	68	16.26	48	0.39
50R-2, 40	509.69	743	3845	0.193	86	15.81	11	0.37
50R-3, 50	510.21	500	792	0.631	65	16.17	43	0.41
				Average:	79		12	

Table T5. Statistical comparison by lithostratigraphic unit of maximum, minimum, average, and standard deviation for values of relative mineral abundance (<2 µm size fraction), Sites C0011 and C0012.

		Abundance in clay-size fraction (SVD normalization factors)																Abundance in bulk smectite (wt%)			
		Smectite (wt%)				Illite (wt%)				Chlorite + Kaolinite (wt%)				Quartz (wt%)							
Lithologic unit	Number of samples	Maximum	Minimum	Average	StDev	Maximum	Minimum	Average	StDev	Maximum	Minimum	Average	StDev	Maximum	Minimum	Average	StDev	Maximum	Minimum	Average	StDev
322-C0011-																					
II	45	96	37	65	14	37	2	24	9	19	0	8	4	14	0	2	3	87	29	42	9
III	58	89	36	59	9	33	10	27	4	19	1	10	4	17	0	4	3	73	31	42	6
IV	44	100	49	68	12	30	0	20	6	20	0	7	5	25	0	5	5	85	25	47	10
V	15	100	45	76	22	34	0	13	14	16	0	4	4	17	0	6	6	91	31	57	22
322-C0012-																					
I	26	81	35	53	10	38	18	32	4	23	1	14	5	9	0	1	2	56	25	36	8
II	17	91	42	63	11	35	9	26	7	16	1	9	4	15	0	2	4	62	26	43	8
III	35	87	38	64	11	35	13	25	5	25	0	8	5	14	0	3	4	62	38	49	7
IV	22	97	49	66	10	25	3	21	5	19	0	8	5	16	0	5	4	87	39	50	10
V	30	97	38	74	14	36	3	18	8	14	0	3	3	14	0	5	6	82	24	50	14

SVD = singular value decomposition. StDev = standard deviation.